termine the attenuation determinants of PV before the development of the transgenic mouse model (37, 41, 56, 65).

Previously, we used defined genetic manipulation to generate an attenuated strain of EV71 (EV71(S1-3′)] that showed a broad spectrum of antigenicity against EV71 strains with attenuated neurovirulence in cynomolgus monkeys (3, 5). The manipulation was based on the temperature-sensitive determinants of the type 1 PV vaccine strain (Sabin 1) located in the conserved regions of enterovirus genome (58); that is, the 5′ nontranslated region (NTR), 3D polymerase gene, and the 3′ NTR (31, 52, 65). In this manipulation, we focused on the attenuation determinants of Sabin 1 but not those of other vaccine strains (Sabin 2 and Sabin 3 strains) for the following reasons: (i) the attenuation determinant of the Sabin 2 strain was in the capsid proteins but not in the 5′ NTR (57; reviewed by Kew [32]); (ii) the attenuation determinant in the 5′ NTR derived from Sabin 3 strain affected the fitness of the EV71 mutant in vitro (5); and (iii) the Sabin 1 strain has shown a high degree of safety, supported in part by the diverse mechanisms of attenuation with many attenuation determinants throughout the genome (52, 53; reviewed by Minor [46]). EV71(S1-3′) showed limited infection in the central nervous system (CNS), where the virus was isolated only from the spinal cords of inoculated monkeys. The tissue specificity of EV71(S1-3′) was different from that of an EV71 mutant [EV71(3′)] which contained the attenuation determinants in the 3D polymerase gene, and the 3′ NTR, and the virus was isolated from the brain stem and the spinal cord (3, 5), suggesting that a cooperative effect of the introduced mutations is required for limited tissue specificity and attenuated neurovirulence of EV71(S1-3′).

To evaluate the effect of the attenuation determinants derived from the type 1 PV vaccine strain, Sabin 1 [PV1(Sabin)], on the virulence of EV71, we developed an adult mouse infection model of EV71 with nonobese-diabetic–severe combined immunodeficiency (NOD/SCID) mice. It has been known that the appearance of neutralizing antibodies directly correlates with the clearance of coxsackie viruses in a mouse infection model (20) and that innate immunity (alpha/beta interferon response) is critical for restricting the apparent tissue specificity of PV infection (26). Therefore, we used NOD/SCID mice to characterize the effect of attenuation determinants on the tissue specificity of EV71 mutants. NOD/SCID mice have defects in innate immunity derived from the phenotype of NOD mice (depression of natural killer activity, a functional deficit in monocytes to secretes cytokines, and absence of C5 activity of complement), which is associated with decreased resistance to herpes virus infection (7, 29, 68), and also have defects in acquired immunity derived from the phenotype of SCID mice (lack of functional B and T cells) (8, 33). We analyzed tissue specificity and age dependency of EV71 mutants with a mouse adaptation mutation and the attenuation determinants of PV1(Sabin) in the CNSs of NOD/SCID mice.

MATERIALS AND METHODS

Cells and viruses. RD cells (derived from human rhabdomyosarcoma) and 293 cells (derived from human embryonic kidney) (18) were cultured as monolayers in Dulbecco's modified Eagle medium (DMEM) supplemented with 10% fetal calf serum (FCS). For the *trans*-encapsidation of EV71 replicons, 293 cells were cultured in serum-free medium (VP-SFM; Gibco) supplemented with 2% FCS.

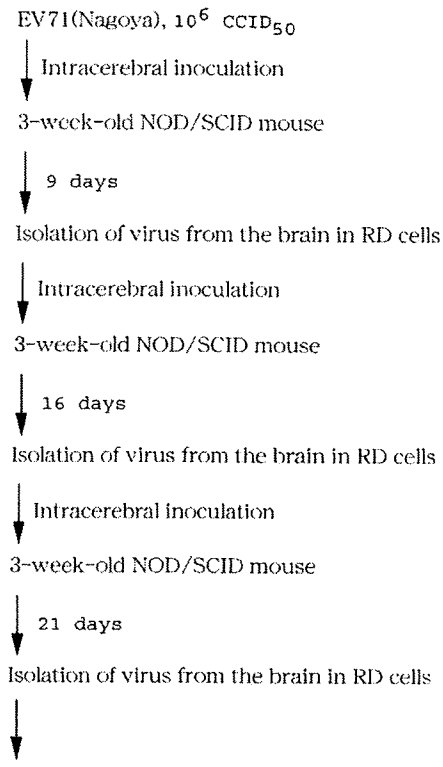

FIG. 1. Adaptation of EV71 in NOD/SCID mice. Three-week-old NOD/SCID mice were inoculated with 10^6 $CCID_{50}$ of EV71(Nagoya) via the intracerebral route. The virus was isolated from the brains of inoculated mice in RD cells. After three rounds of passage, EV71(NOD/SCID) was isolated after limiting dilution in RD cells.

RD cells were used for virus preparation, titration of EV71, and measurement of replication kinetics of EV71 replicon. 293 cells were used for pseudovirus preparation. A mouse-adapted EV71 strain [EV71(NOD/SCID)] was obtained after serial passage of EV71(Nagoya) strain (3, 19) in the brains of NOD/SCID mice (Fig. 1).

General methods of molecular cloning. *Escherichia coli* strain XL10gold (Stratagene) was used for the preparation of plasmids. Ligation of DNA fragments was performed using a quick ligation kit (New England Biolabs). Site-directed mutagenesis (SDM) was performed using KOD Plus DNA polymerase (Toyobo) (59). DNA sequencing was performed using a BigDye Terminator v3.0 cycle sequencing ready reaction kit (Applied Biosystems) and then analyzed with a 3130 genetic analyzer (Applied Biosystems).

Sequence analysis of the genome of the mouse-adapted EV71 strain. The genomic sequence of EV71(NOD/SCID) was determined as described previously (5). Viral genomic RNA was isolated from the culture fluid of infected cells using a High Pure viral RNA kit (Roche). DNA fragments used for DNA sequencing were prepared by reverse transcription-PCR (RT-PCR) using viral genomic RNA as the template by use of a Titan one-tube RT-PCR system (Roche). PCR products were purified using a QIAquick PCR purification kit (Qiagen). The sequences of the 5′ end of the viral genomes were determined using a 5′ rapid-amplification-of-cDNA-ends system, version 2.0 (Invitrogen), according to the manufacturer's instructions. The sequence of the 3′ end of the viral genomes was determined from an RT-PCR product obtained with the primers 7001+ and EcoRI-3END− (Table 1).

Construction of the infectious cDNA clone of mouse-adapted EV71 strains. For the construction of an infectious clone of mouse-adapted EV71 [EV71(NOD/SCID)], a DNA fragment corresponding to nt 1460 to 3444 of EV71(NOD/SCID) was amplified by RT-PCR with the primers *Avr*II-T7-NAGOYA+ and 3602U−. The RT-PCR product was digested by BamHI and NruI and then cloned into the infectious clone of EV71(Nagoya), pEV71(Nagoya) (3). The resultant plasmid was named pEV71(Nagoya-VP231).

TABLE 1. Primers used in this study

Primer	Sequence[a]
2000−	ATTTTACCCGTGGCCATGAATGATC
2876A+	CCCCTACTGGCGAGGTTGTTCCACAATTAC
2876A−	GTAATTGTGGAACAACCTCGCCAGTAGGGG
3164U+	GAACTGTGGGGTCATTGAAATCCAAGTATC
3164U−	GATACTTGGATTTCAATGACCCCACAGTTC
3602U+	GAAGCTAGTGAGTATTTCCCTGCTAGATAC
3602U−	GTATCTAGCAGGGAAATACTCACTAGCTTC
5709+	CGCAACTCTAGTCATCAACACTGAGC
6318A+	GCGCTCTGGGAATCAAAAAAAGAGACATCC
6318A−	GGATGTCTCTTTTTTTGATTCCCAGAGCGC
6399G+	GGGTTGGATCTGCCGTACTCCACTTATG
6399G−	CATAAGTGGAGTACGGCAGATCCAACCC
7001+	GGAGTATGGATTGACCATGACGCCTGCAG
A2*Mlu*I−	AAAAACGCGTTTTTTTTTTTTTTTTTTTTT TTTTTGCTATTCTGG
AUGSacI+	CACGAAGCGATGGGAGCTCAGGTCTCCAC
AUGSacI−	GTGGAGACCTGAGCTCCCATCGCTTCGTG
*Avr*II-T7-NAGOYA+	TTAACCTAGGTTAATACGACTCACTATAGG TTAAAACAGCCTGTGGGTTGTTCC
dSacI+	GATTGAGAGTTCTATAGGAGATAG
dSacI−	CTATCTCCTATAGAACTCTCAATC
d*Sac*I2+	GTGTGGTTCAGAGCCCTAGAGTTGGTTC
d*Sac*I2−	GAACCAACTCTAGGGCTCTGAACCACAC
EcoRI-3END−	ACTGGAATTCTTTTTTTTTTTTTTTTTTT TTTTTV
EGFP-Nagoya+	GGGCCTGACCACCTACGGTTCACAAGTGTC
EGFP-Nagoya−	GACACTTGTGAACCGTAGGTGGTCAGGCCC
Fluc-SacI−	ATTGGAGCTCCAATTTGGACTTTCCGCCC
Nagoya-XbaI−	TTAATCTAGATTAAAGAGTAGTGATGGC
SacI-EV3310+	GGCTGAGCTCAGCCGAACGGCAATCACTAC
SacI-Fluc+	TCAGGAGCTCCTGAAGACGCCAAAAAC
XhoI-EGFP+	TGGTCTCGAGACCATGGGAGCTCTGAGC

[a] Variable sequence position in the primer is expressed according to the IUPAC system. Sequences read from the 5′ position at the left end.

Next, a DNA fragment containing the sequence corresponding to nt 1 to 1460 of EV71(NOD/SCID) was obtained by RT-PCR with the primers *Avr*II-T7-NAGOYA+ and 2000−. The RT-PCR product was digested by AvrII and BamHI and then cloned into pEV71(Nagoya-VP231). The resultant plasmid was named pEV71(Nagoya-VP4231). Finally, the mutations of the EV71(NOD/SCID) genome at nt 3602, 6318, and 6399 were introduced into pEV71(Nagoya-VP4231) by serial SDM with primers containing corresponding mutations (3602U+ and 3602U−, 6318A+ and 6318A−, and 6399G+ and 6399G−, respectively). The resultant plasmid was named pEV71(NOD/SCID). To determine the critical mutation for mouse adaptation, we constructed pEV71(Nagoya-VP231-3164U), pEV71(Nagoya-VP23), and pEV71(Nagoya-2876A) by SDM with primer sets containing corresponding mutations (set 3164U+ and 3164U− and set 2876A+ and 2876A−, respectively).

Preparation of EV71 mutants. RNA transcripts of EV71 mutants were obtained using a RiboMAX large-scale RNA production system-T7 kit (Promega) with AvrII-linearized DNA of EV71 infectious clones as the template. RNA transcripts were transfected into a monolayer of RD cells in six-well plates (Falcon) using a Lipofectamine 2000 reagent (Invitrogen), followed by incubation at 37°C in 10% FCS–DMEM (2 ml per well). The cells were harvested when all the cells exhibited the cytopathic effect and were then stored at −70°C. For the binding assay, EV71(Nagoya) and EV71(Nagoya-2876A) were purified as described below.

Construction of EV71 replicon encoding firefly luciferase. For the construction of an EV71 replicon encoding firefly luciferase (EV71-Fluc mc), we removed two SacI sites on the infectious clone of EV71(BrCr-TR) [pEV71(BrCr-TR)] by serial SDM using two primer sets (set d*Sac*I+ and d*Sac*I− and set d*Sac*I2+ and d*Sac*I2−). The resultant plasmid was named pEV71(d*Sac*I′). Next, to remove a SacI site just after the viral genome on the plasmid, a DNA fragment was obtained by PCR using pEV71(BrCr-TR) as the template with primers 5709+ and A2*Mlu*I− and then cloned into pEV71(d*Sac*I′) following digestion by SpeI and MluI. The resultant plasmid was named pEV71(d*Sac*I). Next, a SacI site was introduced just after the initiation codon of the viral protein-coding region of pEV71(d*Sac*I) by SDM with the primers AUG*Sac*I+ and AUG*Sac*I−. To remove the capsid-coding region of the resultant plasmid, PCR was performed with the primers AUG*Sac*I− and *Sac*I-EV3310+ with the resultant plasmid as the template, and then the PCR product was digested by SacI and subjected to self-ligation. The resultant plasmid was named pEV71(d*Sac*I4). Finally, a DNA fragment encoding firefly luciferase was obtained by PCR using pPV-Fluc mc as the template with primers *Sac*I-Fluc+ and Fluc-*Sac*I− (4) and then cloned into pEV71(d*Sac*I4) following digestion by SacI. The resultant plasmid was named pEV71(Fluc-mc).

Construction of EV71 capsid-expressing vectors. For the construction of an expression vector of EV71(Nagoya) capsid proteins, we first fused the enhanced green fluorescence protein (EGFP) gene to the EV71 capsid protein coding region by PCR. The EGFP coding region and the EV71 capsid protein coding region were amplified by PCR with *Xho*I-EGFP+ and EGFP-Nagoya− and with EGFP-Nagoya+ and Nagoya-*Xba*I− using pIRES2-EGFP (Clontech) and pEV71(Nagoya) as templates (3), respectively. Next, these DNA fragments were fused by PCR using the primers *Xho*I-EGFP+ and Nagoya-*Xba*I− and then cloned into the pKS435 expression vector (a kind gift from Koji Sakai, AIDS Research Center, National Institute of Infectious Diseases, Tokyo, Japan), which was useful for the expression of PV capsid proteins (4), following digestion by XhoI and XbaI. The resultant plasmid was named pKS435-EGFP-EV71(Nagoya) capsid. For the analysis of mouse-adapted EV71, a mutation at nt 2876 (change of guanine to adenine) was introduced into pKS435-EGFP-EV71(Nagoya) capsid by SDM with the primers 2876A+ and 2876A−. The resultant plasmid was named pKS435-EGFP-EV71(Nagoya-2876A) capsid. These capsid expression vectors were used for the *trans*-encapsidation of the EV71 replicon.

DNA transfection. A six-well plate (Falcon) with a 30% confluent monolayer of 293 cells was transfected with 1 μg of DNA of pKS435-EGFP-EV71(Nagoya) capsid or pKS435-EGFP-EV71(Nagoya-2876A) capsid per well using a Lipofectamine 2000 reagent (Invitrogen) and then incubated at 37°C in 2 ml per well of 10% FCS–DMEM. The cells were washed with 10% FCS–DMEM at 3 h posttransfection and then used for the *trans*-encapsidation of the EV71 replicon.

***trans*-encapsidation of the EV71 replicon.** For the preparation of *trans*-encapsidated EV71-Fluc mc (TE-EV71-Fluc mc), the RNA transcript of the EV71 replicon was obtained with AvrII-linearized DNA of pEV71-Fluc mc as the template and transfected into a monolayer of 293 cells in six-well plates (Falcon) which transiently expressed EV71 capsid proteins using a Lipofectamine 2000 reagent (Invitrogen), and cells were then incubated at 37°C in 2% FCS–VP-SFM (2 ml per well). The cells were harvested 24 h posttransfection and stored at −70°C.

Virus purification. After freezing and thawing of the harvested cells, EV71 and pseudoviruses were purified from the infected cells using DEAE-Sepharose CL-6B (Amersham Pharmacia Biotech) as described previously (2), followed by centrifugation at 35,000 rpm for 2.5 h at 4°C in a Beckman SW41 rotor with 1 ml of 30% sucrose cushion. The pellet was washed three times with distilled water and then dissolved in 100 μl of phosphate-buffered saline (PBS) with calcium and magnesium (PBS+; 9.6 mM phosphate buffer [pH 7.4], 137 mM NaCl, 2.6 mM KCl, 0.49 mM $MgCl_2$, 0.9 mM $CaCl_2$) at 4°C overnight. The pellet was dissolved by pipetting and then stored at −70°C.

Real-time TaqMan PCR. Real-time TaqMan PCR for the detection of the EV71 genome was performed as previously described by Nijhuis et al. (51). Briefly, viral RNA was isolated from 10% (wt/vol) tissue homogenate in DMEM containing 10% FCS or from serum, which was diluted 1,000-fold with HEPES-buffered saline (HeBS; 21 mM HEPES buffer [pH 7.4], 1.8 mM phosphate, 137 mM NaCl, and 4.8 mM KCl), of infected mice using a High Pure viral RNA purification kit (Roche). The isolated RNA was reverse transcribed using a reverse transcription system (Promega) with random hexamers according to the manufacturer's instructions. The resultant cDNA was assayed in a 20-μl reaction mixture containing 2 μl cDNA solution and 10 μl of TaqMan fast universal PCR master mix (Applied Biosystems) with a forward primer, reverse primer 1, and probe 1 (51). Plasmid DNA of an EV71 infectious clone [pEV71(Nagoya)] was used to control the quantification of the number of copies. The mixtures were subjected to real-time PCR; the PCR conditions consisted of a denaturation step at 95°C for 20 s and 40 cycles of thermal cycling of 95°C for 3 s and 60°C for 30 s. The fluorescence emission of the probe was monitored and analyzed using a 7500 fast real-time PCR system (Applied Biosystems).

Luciferase assay. RD cells in 96-well plates (Falcon) (2.8×10^4 cells per well in 100 μl of Eagle's minimum essential medium supplemented with 2% FCS) were inoculated with 50 μl of the indicated number of copies of TE-EV71(Nagoya)-Fluc mc or TE-EV71(Nagoya-2876A)-Fluc mc and were then incubated at 37°C for 2 h (see Fig. 3C). The cells were washed three times with 10% FCS–DMEM and were then added to 100 μl of 10% FCS–DMEM followed

by incubation at 37°C. The cells were harvested at the indicated times (see Fig. 3C) by adding 30 μl of passive lysis buffer (Promega). Part of the lysate (2 μl) was used for the measurement of luciferase activity. Luciferase activity was measured with a luciferase assay system (Promega) using a TR717 microplate luminometer (Applied Biosystems) according to the manufacturer's instructions.

Electron microscopy. Purified TE-EV71-Fluc mc was subjected to negative staining in uranyl acetate as described previously (67). Samples were examined under transmission electron microscopy (JEM-1220; JEOL Datum) at an acceleration voltage of 80 kV, and the images were obtained at a magnification of ×50,000.

Binding assay. RD cells in 24-well plates (Falcon) (2.2×10^5 cells) were inoculated with 150 μl of 10% FCS–DMEM containing the indicated numbers of copies of purified EV71(Nagoya) or EV71(Nagoya-2876A) in the presence of 2 mM guanidine hydrochloride and were then incubated at room temperature for 30 min (see Fig. 3D). The cells were washed three times with 10% FCS–DMEM and then harvested by adding 100 μl of HeBS containing 2% *N*-lauroylsarcosine. Viral RNA was extracted from the collected cell lysate, and then the number of copies of the viral genome in the cell lysate was determined by real-time TaqMan PCR.

Virus titration. Virus titer was determined by measuring 50% cell culture infective dose ($CCID_{50}$) by microtitration assay in RD cells for EV71 (50) and also by measuring the infectious units (IU) by counting the number of the infected cells stained by the indirect immunofluorescence against firefly luciferase expressed by pseudovirus (4, 6). For the measurement of $CCID_{50}$, virus solution was inoculated into an RD cell suspension on 96-well plates (Falcon) and then incubated at 35°C for 1 week for the observation of cytopathic effect. The $CCID_{50}$ was calculated according to the Behrens-Kärber method (28). For the measurement of IU, pseudovirus solution was diluted with 10% FCS–DMEM and inoculated into RD cell monolayers on 96-well plates (Falcon) (2.8×10^4 cells per well). The cells were incubated at 37°C for 10 h and then fixed with 3% paraformaldehyde. The cells were stained by indirect immunofluorescence with rabbit anti-firefly luciferase antibody (1:100 dilution with 0.1% Triton X-100 in PBS without calcium and magnesium [PBS−]; Cortex Biochem) (1). The number of infected cells was counted for the calculation of IU (27).

Intracerebral inoculation and histological analysis of NOD/SCID mice. All animal procedures were approved by the Committee for Biosafety and Animal Handling and the Committee for Ethical Regulation of the National Institute of Infectious Diseases, Japan. Animal care, breeding, virus inoculation, and observation were performed in accordance with the guidelines of the committees.

NOD/SCID mice (NOD.CB17-*Prkdc*^{scid}/J strain, 3 or 4 weeks old; The Jackson Laboratory) were inoculated with 10^6 $CCID_{50}$ of EV71 mutants via the intracerebral route or with $10^{6.5}$ $CCID_{50}$ of EV71(Nagoya-2876A) via the intravenous route. Inoculated mice were observed for up to 1 month for clinical symptoms (paralysis and death). Mice were sacrificed when paralysis was observed or at 1 month postinoculation (p.i.). For quantification of viral genome in tissues, a portion of excised tissue was stored at −70°C. After freezing and thawing, 10% (wt/vol) tissue homogenates in 10% FCS–DMEM were prepared and centrifuged at 10,000 × *g* for 10 min to remove cell debris. Supernatants were diluted 10-fold with HeBS and then subjected to RNA extraction. For histological analysis, the tissues of inoculated mice were collected at 4 weeks p.i., and sections of each tissue were prepared. The lesions on the sections were observed after hematoxylin-and-eosin staining. The viral antigen was detected on sections as described previously (48). Sections were deparaffinized with xylene, rehydrated in ethanol, and then treated with 0.25% trypsin solution with 0.5% $CaCl_2$ in PBS− for 30 min and incubated in 1% hydrogen peroxide in methanol to block endogenous peroxidase activity followed by incubation with 10% Block Ace (DS Pharma Biomedical Co., Ltd.) in PBS−. The treated sections were incubated with anti-EV71(C7-Osaka) hyperimmune serum (1:1,000 dilution with 0.1% Triton X-100-PBS−) at 4°C overnight. After three washes with PBS−, the sections were incubated with biotin-conjugated anti-rabbit immunoglobulin G for 30 min at 37°C and then incubated with streptavidin-peroxidase. The peroxidase activity was developed in diaminobenzidine with hydrogen peroxide. The section was counterstained with hematoxylin to stain the nuclei.

Temperature sensitivity. RD cells (1.9×10^5 cells) were inoculated with each virus at a multiplicity of infection of 1 and then incubated at 36°C or at 39°C for 2 h. The cells were washed three times at 2 h p.i., and then 0.5 ml of 10% FCS–DMEM was added to the cells. The cells were incubated at 36°C or at 39°C for 8 h (10 h p.i.) and then stored at −70°C. After freezing and thawing, the viral RNA was extracted from the cell lysate, and then the number of copies of viral RNA was determined using real-time PCR.

RESULTS

Isolation and characterization of a mouse-adapted EV71 strain in NOD/SCID mice. To obtain EV71(NOD/SCID), 3-week-old NOD/SCID mice were inoculated with EV71 (Nagoya) via the intracerebral route, and then the brains were collected and the homogenates were inoculated to RD cells to amplify the virus for the next passage in NOD/SCID mice (Fig. 1). In the third passage, inoculated mice showed paralysis of the hind limbs. Virus was isolated from the paralyzed mice and then purified by limiting dilution in RD cells [EV71(NOD/SCID)]. Sequence analysis of the viral genome showed 16 mutations relative to the parental EV71(Nagoya) genome (Fig. 2A). Among the mutations, one at nt 2876 (a change of guanine to adenine) that caused an amino acid change of glycine to glutamic acid at amino acid position 145 of VP1 capsid protein was sufficient to confer the mouse-adapted phenotype on the parental EV71(Nagoya) (Fig. 2).

Mutation at nt 2876 of EV71 affected binding of the virion to RD cells. To characterize the effect of the mutation at nt 2876 on EV71 infection, we analyzed the early steps of the infection (binding and uncoating steps) of EV71 mutant with the mutation in human RD cells, because EV71(NOD/SCID) could not infect mouse L cells (data not shown).

First, we analyzed the uncoating step of the *trans*-encapsidated EV71 replicons, with or without the mutation, at amino acid position 145 of VP1 protein [TE-EV71(2876A)-Fluc mc and TE-EV71-Fluc mc] (Fig. 3). The titer of TE-EV71-Fluc mc was 1.8×10^5 IU per ml, which was about 2 log lower than that of PV pseudovirus (6.3×10^7 IU per ml) (4). After purification of the pseudovirus, the amount of nonencapsidated viral RNA in the sample was negligible ($<1/10^5$ of the amount of *trans*-encapsidated RNA) (Fig. 3A and B). The replication kinetics of the pseudoviruses were similar, and no lag time caused by delayed uncoating was observed (Fig. 3C). However, the infectivity of TE-EV71(2876A)-Fluc mc was 10-fold lower than that of TE-EV71-Fluc mc.

Next, we analyzed the binding of EV71 virions to RD cells. The titer of EV71(Nagoya-2876A), which has a mouse adaptation mutation at nt 2876, was slightly reduced compared with that of the parental EV71(Nagoya) (10^8 $CCID_{50}$/ml and $10^{8.625}$ $CCID_{50}$/ml, respectively). EV71(Nagoya-2876A) showed a markedly decreased level of binding to RD cells (45-fold) compared with the parental EV71(Nagoya).

These results indicated that the mouse adaptation mutation at nt 2876 affected virus binding in RD cells.

Tissue specificity of mouse-adapted EV71 in NOD/SCID mice. We examined the tissue specificity of an EV71 mutant with mouse adaptation mutation [EV71(Nagoya-2876A)] in NOD/SCID mice. We used a real-time TaqMan PCR method for the detection of the viral RNA because the virus titer in the tissue homogenate was not high enough to be detected by microtitration assay (2.5×10^3 [cerebellum] to 3.8×10^4 [heart] copies of viral RNA per $CCID_{50}$). The numbers of copies per $CCID_{50}$ of EV71 mutants prepared as cell lysates were around 10^3 (Table 2). After intracerebral inoculation with EV71(Nagoya-2876A), we detected the viral RNA in the CNS and in serum at 1 week p.i. (Fig. 4A). At 3 to 4 weeks p.i., a high copy number of viral RNA was detected in the heart and the skeletal muscle as well as in the spinal cord. Viral RNA was

(A)

Nucleotide change	Site of mutation	Amino acid change
584 U(Nagoya) to C(NOD/SCID)	5'NTR	-
602 A(Nagoya) to G(NOD/SCID)	5'NTR	-
736 A(Nagoya) to G(NOD/SCID)	5'NTR	-
930 C(Nagoya) to U(NOD/SCID)	VP4	-
1573 U(Nagoya) to C(NOD/SCID)	VP2	-
1662 C(Nagoya) to U(NOD/SCID)	VP2	-
2005 G(Nagoya) to C(NOD/SCID)	VP3	VP3 97:E(Nagoya) to Q(NOD/SCID)
2244 C(Nagoya) to U(NOD/SCID)	VP3	-
2396 G(Nagoya) to A(NOD/SCID)	VP3	VP3 227:R(Nagoya) to K(NOD/SCID)
2416 C(Nagoya) to G(NOD/SCID)	VP3	VP3 234:H(Nagoya) to D(NOD/SCID)
2488 A(Nagoya) to G(NOD/SCID)	VP1	VP1 16:M(Nagoya) to V(NOD/SCID)
2876 G(Nagoya) to A(NOD/SCID)	VP1	VP1 145:G(Nagoya) to E(NOD/SCID)
3164 U(Nagoya) to C(NOD/SCID)	VP1	VP1 241:L(Nagoya) to S(NOD/SCID)
3602 A(Nagoya) to U(NOD/SCID)	2A	2A 90:Y(Nagoya) to F(NOD/SCID)
6318 G(Nagoya) to A(NOD/SCID)	3D	-
6399 A(Nagoya) to G(NOD/SCID)	3D	-

(B)

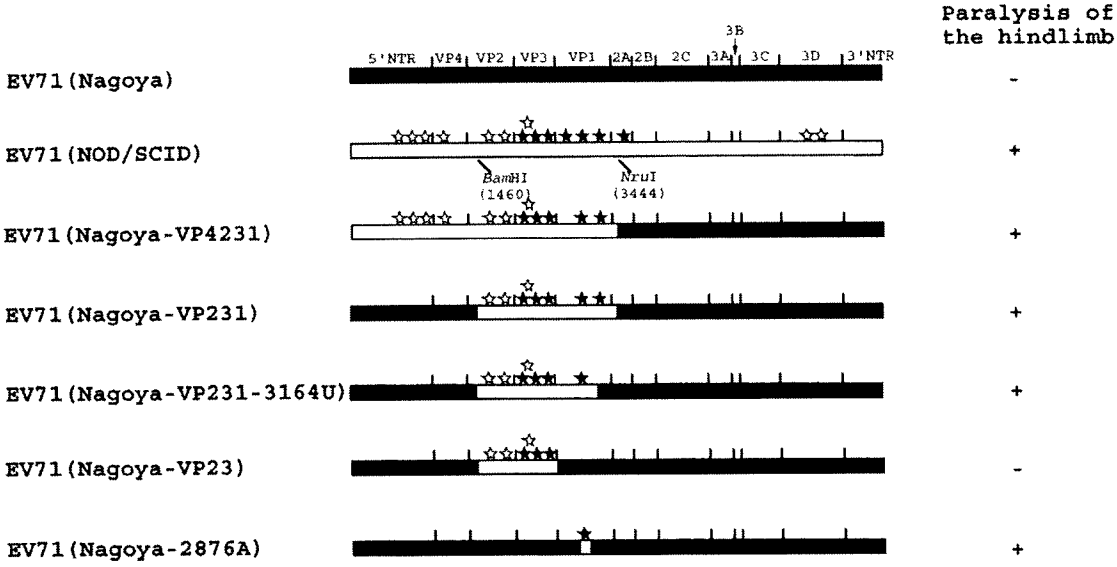

FIG. 2. Identification of the mouse adaptation determinant of EV71(NOD/SCID). (A) Nucleotide and amino acid changes from the parental EV71(Nagoya) to EV71(NOD/SCID). (B) Mouse-adapted phenotypes of EV71 mutants with mouse adaptation mutations. Sequences derived from the parental EV71(Nagoya) genome are represented by the closed regions, and the synonymous and nonsynonymous mutations derived from EV71(NOD/SCID) are represented by the open regions with white and black stars, respectively, above them. + and −, EV71 mutants that did and did not cause paralysis in inoculated mice, respectively.

also detected in other extraneural tissues (lung, liver, spleen, and kidney) along with an increased level of viremia. The preferential virus distribution to the heart observed at 3 and 4 weeks p.i. was also observed at 24 h p.i. after intravenous inoculation (Fig. 4A). The viral antigen was detected only in the heart and the skeletal muscle of inoculated NOD/SCID mice, not in other tissues (Fig. 4B). These results suggest that, along with the CNS, the heart and the skeletal muscle are the major infection sites of a mouse-adapted EV71 strain in NOD/SCID mice.

Effect of attenuation determinants derived from PV1(Sabin) on EV71 infection in NOD/SCID mice. We examined the effects of attenuation determinants derived from PV1(Sabin) on virulence and tissue specificity of EV71(Nagoya-2876A). EV71 mutants containing these determinants showed temperature sensitivity, as previously observed for those constructed based on strain BrCr-TR (5) (Table 3). Minor temperature sensitivity was conferred on the EV71(Nagoya-2876A-S1) mutant by the determinant in the 5′ NTR, and strong temperature sensitivity was conferred on the EV71(Nagoya-2876A-3′) and EV71 (Nagoya-2876A-S1-3′) mutants by the determinants in the 3D polymerase-coding region and in 3′ NTR.

In 3-week-old mice, the effects of individual determinants in the 5′ NTR, 3D polymerase region, and 3′ NTR were weak and could not suppress paralysis in mice inoculated with EV71 mutants (Fig. 5A). However, when all the determinants were introduced into EV71(Nagoya-2876A), the mutant EV71 (Nagoya-2876A-S1-3′) showed drastic reduction in replication (Fig. 5B). The reduction was especially evident in the skeletal muscle and other extraneural tissues, although the levels of

(A)

Pseudovirion	Copy number of viral genomic RNA (in 5 μl)
TE-EV71-Fluc mc	1.2×10^8
TE-EV71(2876A)-Fluc mc	2.5×10^8
EV71-Fluc mc(without capsid)	6.8×10^2

(B)

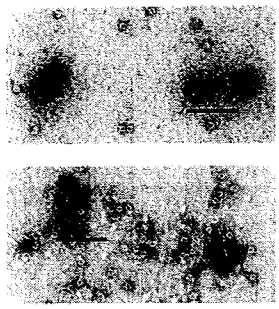

TE-EV71-Fluc mc

TE-EV71(2876A)-Fluc mc

(C)

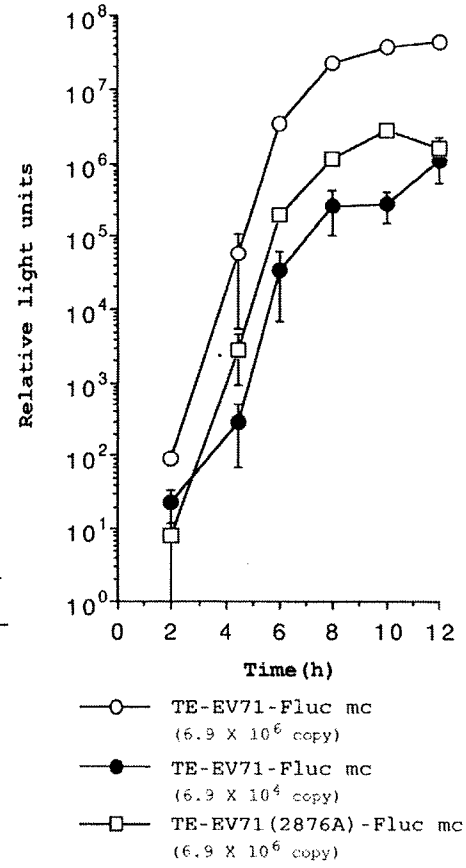

(D)

Virion	Amount of virion added to cells	Amount of virion bound to cells	Binding activity (%)
EV71(Nagoya)	2.1×10^9	$2.9(1.3) \times 10^6$	100
	2.1×10^8	$1.5(0.44) \times 10^5$	100
EV71(Nagoya-2876A)	2.1×10^9	$6.4(1.6) \times 10^4$	2.2
	2.1×10^8	$3.0(1.5) \times 10^3$	2.0

FIG. 3. Effect of mouse adaptation mutation at nt 2876 on EV71 infection in RD cells. (A) Purification of EV71 pseudovirions. The number of copies of viral RNA in purified TE-EV71-Fluc mc and TE-EV71(2876A)-Fluc mc pseudovirions was determined by real-time PCR. The amount of nonencapsidated viral RNA in the sample was determined from samples prepared from 293 cells that were not pretransfected with the DNA of pKS435-EGFP-EV71(Nagoya) capsid vector for capsid proteins expression before RNA transfection with RNA transcript of EV71-Fluc mc. (B) Electron microscopy observation of purified EV71 pseudovirions. Bar, 100 nm. (C) Replication kinetics of EV71 replicon in RD cells infected with pseudovirions. RD cells (1.4×10^4 cells) were infected with 6.9×10^4 to 6.9×10^6 pseudovirions. The cells were washed at 2 h p.i., and then the luciferase activity in the cells was measured at the indicated times. Total luciferase activity with standard deviations is shown. (D) Binding of mouse-adapted EV71 mutant to RD cells. EV71(Nagoya) or EV71(Nagoya-2876A) virions were incubated with RD cells at room temperature for 30 min in the presence of 2 mM guanidine hydrochloride. The amount of virions bound to RD cells was determined by real-time PCR. The binding activity of EV71(Nagoya) was taken as 100%.

viremia were comparable among mice inoculated with the different mutants. Therefore, the cooperative effect of the determinants was critical for the attenuation of EV71 in 3-week-old mice.

TABLE 2. Copy numbers of viral RNA per $CCID_{50}$ of EV71 mutants

EV71 strain	No. of copies of viral genome (in 100 μl)[a]	$CCID_{50}$ (in 100 μl)	No. of copies of viral genome/ $CCID_{50}$
BrCr-TR	3.3×10^9	3.1×10^6	1.1×10^3
Nagoya	3.4×10^9	1.8×10^7	1.9×10^2
Nagoya-2876A	2.0×10^{10}	5.6×10^6	3.6×10^3
Nagoya-2876A-S1	1.7×10^{10}	4.8×10^6	3.5×10^3
Nagoya-2876A-3′	1.8×10^{10}	2.4×10^6	7.5×10^3
Nagoya-2876A-S1-3′	1.4×10^{10}	2.4×10^6	5.8×10^3

[a] Viral RNA was extracted from each virus solution (prepared as crude cell lysates of infected RD cells), and then the number of copies of viral RNA was determined using real-time PCR.

In 4-week-old mice, the effects of individual determinants appeared to be stronger than those observed in 3-week-old mice. Each mutant showed attenuated phenotypes associated with decreased levels of virus replication in the tissues (Fig. 5C). The replication of EV71(2876A-3′) was more severely affected than that of EV71(2876A-S1).

These results suggest that factors required for apparent attenuation depend on the age of the animal and that a cooperative effect of the attenuation determinants is critical for the attenuation of EV71 in NOD/SCID mice.

DISCUSSION

In this study, we established a mouse model of EV71 infection in 3- to 4-week-old NOD/SCID mice with mouse-adapted mutants of EV71(Nagoya). NOD/SCID mice showed a prolonged EV71 infection (>1 month) with broad tissue specificity, possibly supported by the lack of the production of anti-

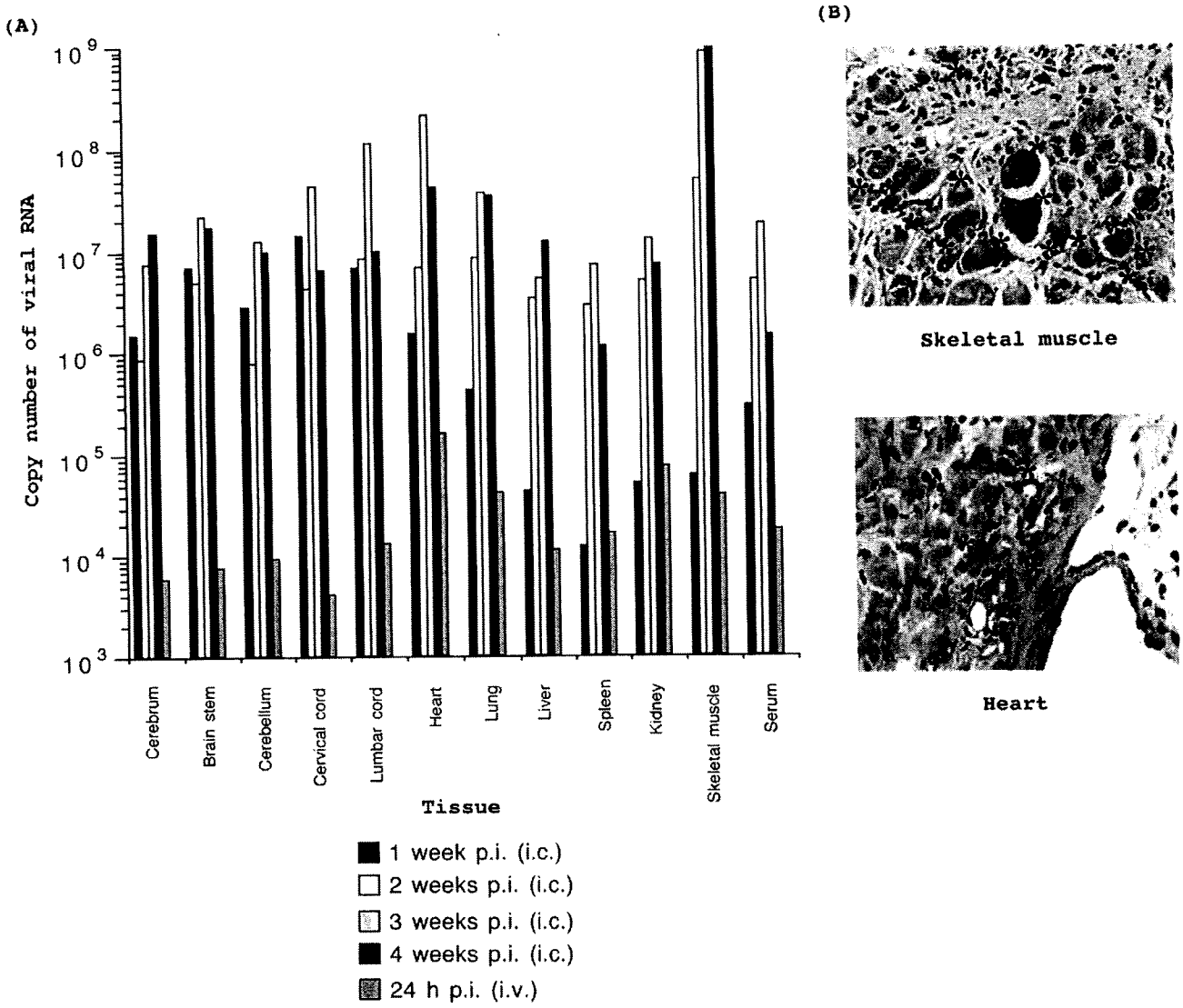

FIG. 4. Infection of NOD/SCID mice with EV71(Nagoya-2876A). (A) Time course of virus dissemination in NOD/SCID mice after intracerebral inoculation. NOD/SCID mice were inoculated with 10^6 $CCID_{50}$ of EV71(Nagoya-2876A) via the intracerebral route, and then the tissues were collected at the time indicated. To determine the primary infection sites after the establishment of viremia, NOD/SCID mice were inoculated with $10^{6.5}$ $CCID_{50}$ of EV71(Nagoya-2876A) via the intravenous route, and then the tissues were collected at 24 h p.i. The number of copies of viral RNA in each tissue was determined by real-time PCR. The number of copies of viral RNA in 0.1 g of each tissue or in 5 μl of serum are shown. (B) Detection of viral antigen in NOD/SCID mice. The viral antigen was detected in the skeletal muscles and hearts of infected mice. The cells with viral antigen are shown with an asterisk.

EV71 antibody in NOD/SCID mice (Fig. 4) (20). The permissive age of NOD/SCID mice for mouse-adapted EV71 infection (>3 weeks old) was higher than the permissive ages of the reported mouse infection models with normal mice (1 to 7 days old) (14, 71). We identified a mutation at nt 2876 that caused a single amino acid change of VP1 at amino acid position 145 as the determinant of mouse adaptation of EV71(Nagoya) (Fig. 2). This amino acid residue is located at around the fivefold axis on the surface of the EV71 virion, according to a structure model calculated from the crystal structure of bovine enterovirus (63). However, mouse-adapted EV71 strains and EV71 pseudoviruses with the mouse adaptation determinant at nt 2876 could not infect mouse L cells. When the in vitro-synthesized RNA transcript of EV71 replicon was transfected into mouse L cells, vigorous replication was observed (M. Arita, unpublished observation). Therefore, it is plausible that isolated mouse-adapted strains could not infect mouse L cells because of the lack of a receptor on the cells. The number of copies of the pseudovirions were similar with and without the mutation at nt 2876, suggesting encapsi-

TABLE 3. Temperature sensitivity of EV71 mutants

EV71 strain	No. of copies		Δ 36/39°C[a]
	36°C	39°C	
Nagoya-2876A	1.6×10^9	1.0×10^9	0.2
Nagoya-2876A-S1	1.1×10^9	3.0×10^8	0.6
Nagoya-2876A-3'	8.3×10^7	2.0×10^5	2.6
Nagoya-2876A-S1-3'	2.1×10^8	8.0×10^4	3.4

[a] Log_{10} ratio of the numbers of copies observed at 36 and 39°C.

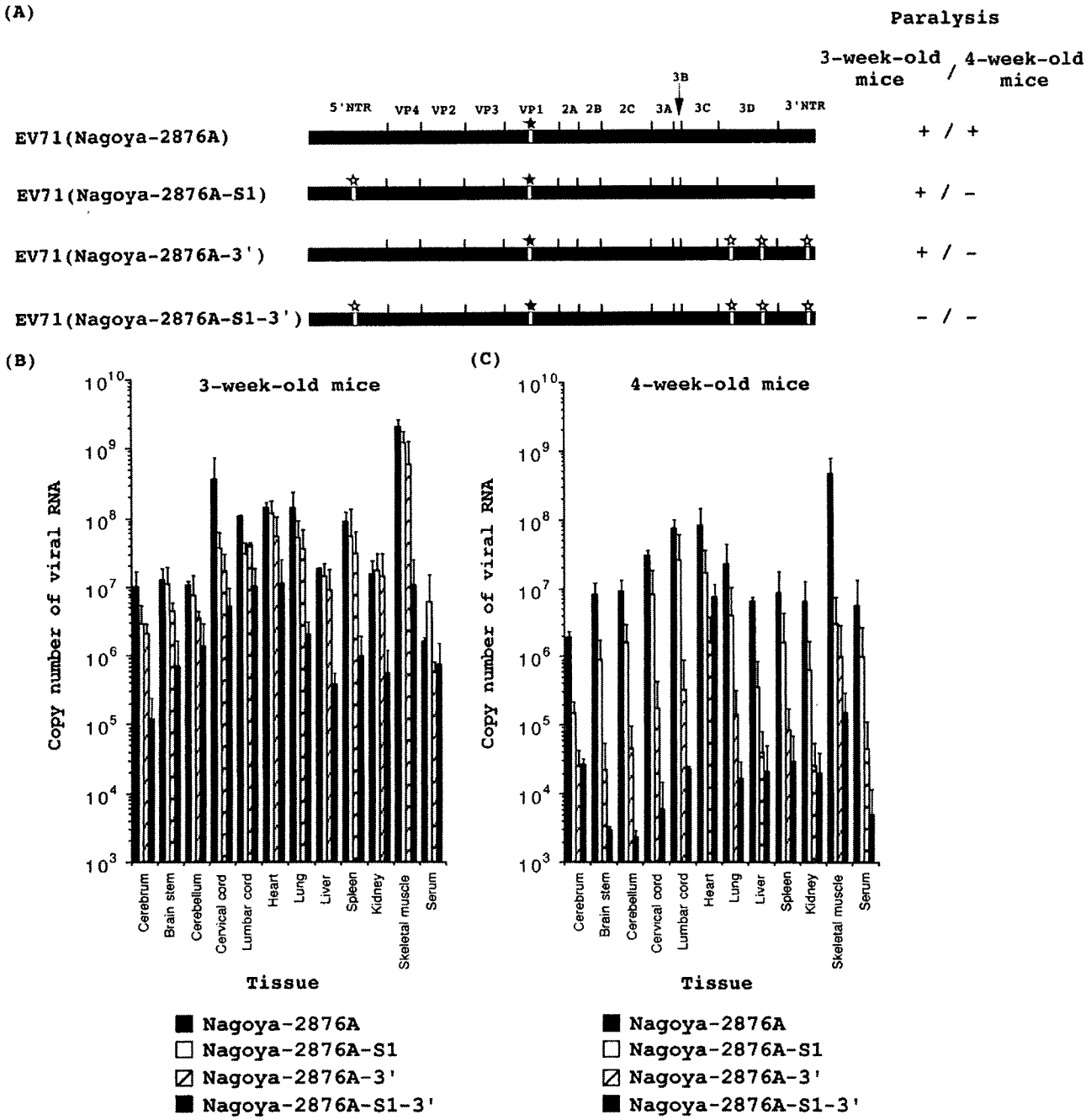

FIG. 5. Characterization of the effect of the attenuation determinants of PV1(Sabin) on EV71 infection in NOD/SCID mice. (A) Mouse-adapted phenotype of EV71(Nagoya-2876A) with the attenuation determinants of PV1(Sabin). The sequences derived from the parental EV71(Nagoya) genome are represented by the closed regions, and the introduced mutations are represented by the open regions with stars above them. White stars represent the attenuation determinants of PV1(Sabin) and black stars represent a mouse adaptation mutation derived from EV71(NOD/SCID) at nt 2876. + and −, EV71 mutants that did and did not cause paralysis, respectively, in the inoculated mice (3 and 4 weeks old). (B and C) Tissue specificity of EV71 mutants in 3- and 4-week-old NOD/SCID mice. NOD/SCID mice were inoculated with 10^6 $CCID_{50}$ of each mutant via the intracerebral route, and the tissues were collected when the mice showed paralysis or at 4 weeks p.i. The number of copies of viral RNA in each tissue was determined by real-time PCR. The number of copies of viral RNA in 0.1 g of each tissue or in 5 μl of serum is shown.

dation was not the target step of the mutation for mouse adaptation (Fig. 3A). The mutation at nt 2876 affected the virion binding (Fig. 3D). The thermostability of EV71(Nagoya-2876A) examined in the range of 37 to 47°C was comparable to that of the parental strain EV71(Nagoya) (data not shown), which is considered important for the mouse adaptation of PV with enhanced uncoating efficiency (17). The mutation at nt 2876 might increase the efficiency of uncoating upon

specific binding of the virion to the receptor molecule on the target cells in NOD/SCID mice, although the increase in the uncoating efficiency observed in human RD cells was at most 4.5-fold (Fig. 3C and D). These observations suggest that the primary effect of the mouse adaptation mutation is on the enhancement of the virion binding to the target cells in NOD/SCID mice to facilitate the infection of the mouse-adapted EV71 strain.

We observed broad tissue specificity of mouse-adapted EV71 in NOD/SCID mice (Fig. 4). The inoculated NOD/SCID mice showed paralysis of the hind limbs at 2 to 4 weeks p.i. but not of the forelimbs, although a similar level of replication was observed in the cervical and the lumbar spinal cords after intracerebral inoculation (Fig. 4 and 5; also data not shown). Among the tissues examined, along with the CNS, the heart and the skeletal muscle were the major targets of EV71 infection in NOD/SCID mice. Abundant viral-antigen-positive cells were observed in the skeletal muscles of the hind limbs, showing atrophic polymyositis with degeneration of the muscle cells and proliferation of fibroblasts in the interstitial tissue, while only a few muscle cells were positive in the heart (Fig. 4A). In contrast, we observed no lesions and no dissolution of neurons in the brain stem and lumbar spinal cord (data not shown). In humans and monkeys, the major infection sites of EV71 were in the brain stem and the spinal cord (3, 40, 49, 50). Therefore, the tissue specificity of a mouse-adapted EV71 strain in NOD/SCID mice was different from specificities in humans and monkeys. Interestingly, the observed tissue specificity of an EV71 mutant with a mouse adaptation determinant [EV71(Nagoya-2876A)] showed a good correlation with the viral internal ribosomal entry site activities in mice (30). This suggests that the tissue specificity of EV71(Nagoya-2876A) was determined after the step of virus binding to the target cells in NOD/SCID mice. The viral antigen was detected in the heart and skeletal muscle but not in the CNS tissues of NOD/SCID mice (Fig. 4B). Muscle tissues are hard to homogenize compared with CNS tissues. Therefore, the virus titer in muscle tissues might have been underestimated by inefficient extraction of the viral RNA from these tissues. In a mouse infection model of EV71 using 7-day-old mice, the muscle contained the highest titer of virus, and the limb muscles displayed massive necrosis from the infection (71). Therefore, the observed paralysis of the hind limbs in NOD/SCID mice might be caused by polymyositis and not by the lesion in the CNS. The target cells of EV71(Nagoya-2876A) in NOD/SCID mice need to be determined in future studies.

A cooperative effect of the attenuation determinants of PV1(Sabin) on the attenuation of PV has been observed in monkey and mouse infection models (9, 24, 43, 52, 65), and in a monkey model of EV71 infection (3, 5). We observed that the cooperative attenuation effect on EV71 infection in NOD/SCID mice was age independent (Fig. 5). However, individual effects of the determinants were age dependent. The determinants of PV1(Sabin) in the 3D polymerase and 3′ NTR, which are known as strong temperature-sensitive determinants (5, 9), conferred an attenuated phenotype on EV71 in 4-week-old mice but not in 3-week-old mice. This suggests that temperature sensitivity could be the dominant factor for attenuation in adult mice. In fact, an attenuation determinant in the 5′ NTR of PV3(Sabin), which served as a major attenuation determinant in adult mice (4 weeks old) but not in newborn mice (1 to 2 days old), has been reported (30). These results indicate that the cooperative effect of the attenuation determinants is critical for the attenuation of EV71 in NOD/SCID mice.

The tissue specificities of EV71 mutants examined in this study were similar in the CNS, suggesting that the introduced determinants had no effect on the tissue specificity of EV71 in the CNS. This suggests that the neuroattenuated phenotype of EV71(S1-3′) in the brain stems of cynomolgus monkeys was conferred by a non-tissue-specific cooperative effect of the determinants.

In summary, we developed an NOD/SCID mouse model of EV71 infection and characterized the effect of the attenuation determinants of PV1(Sabin) on the attenuation of EV71 in NOD/SCID mice. The results suggest that a cooperative effect of attenuation determinants is critical for attenuation of EV71.

ACKNOWLEDGMENTS

We are grateful to Junko Wada for her excellent technical assistance.

This study was supported by Grants-in-Aid from the Japan Society for Promotion of Science and for Research on Emerging and Re-emerging Infectious Diseases from the Ministry of Health, Labor and Welfare.

REFERENCES

1. **Arita, M., H. Horie, M. Arita, and A. Nomoto.** 1999. Interaction of poliovirus with its receptor affords a high level of infectivity to the virion in poliovirus infections mediated by the Fc receptor. J. Virol. **73**:1066–1074.
2. **Arita, M., S. Koike, J. Aoki, H. Horie, and A. Nomoto.** 1998. Interaction of poliovirus with its purified receptor and conformational alteration in the virion. J. Virol. **72**:3578–3586.
3. **Arita, M., N. Nagata, N. Iwata, Y. Ami, Y. Suzaki, K. Mizuta, T. Iwasaki, T. Sata, T. Wakita, and H. Shimizu.** 2007. An attenuated strain of enterovirus 71 belonging to genotype A showed a broad spectrum of antigenicity with attenuated neurovirulence in cynomolgus monkeys. J. Virol. **81**:9386–9395.
4. **Arita, M., N. Nagata, T. Sata, T. Miyamura, and H. Shimizu.** 2006. Quantitative analysis of poliomyelitis-like paralysis in mice induced by a poliovirus replicon. J. Gen. Virol. **87**:3317–3327.
5. **Arita, M., H. Shimizu, N. Nagata, Y. Ami, Y. Suzaki, T. Sata, T. Iwasaki, and T. Miyamura.** 2005. Temperature-sensitive mutants of enterovirus 71 show attenuation in cynomolgus monkeys. J. Gen. Virol. **86**:1391–1401.
6. **Barclay, W., Q. Li, G. Hutchinson, D. Moon, A. Richardson, N. Percy, J. W. Almond, and D. J. Evans.** 1998. Encapsidation studies of poliovirus subgenomic replicons. J. Gen. Virol. **79**:1725–1734.
7. **Baxter, A. G., and A. Cooke.** 1993. Complement lytic activity has no role in the pathogenesis of autoimmune diabetes in NOD mice. Diabetes **42**:1574–1578.
8. **Bosma, G. C., R. P. Custer, and M. J. Bosma.** 1983. A severe combined immunodeficiency mutation in the mouse. Nature **301**:527–530.
9. **Bouchard, M. J., D. H. Lam, and V. R. Racaniello.** 1995. Determinants of attenuation and temperature sensitivity in the type 1 poliovirus Sabin vaccine. J. Virol. **69**:4972–4978.
10. **Brown, B. A., and M. A. Pallansch.** 1995. Complete nucleotide sequence of enterovirus 71 is distinct from poliovirus. Virus Res. **39**:195–205.
11. **Chang, L. Y., T. Y. Lin, K. H. Hsu, Y. C. Huang, K. L. Lin, C. Hsueh, S. R. Shih, H. C. Ning, M. S. Hwang, H. S. Wang, and C. Y. Lee.** 1999. Clinical features and risk factors of pulmonary oedema after enterovirus-71-related hand, foot, and mouth disease. Lancet **354**:1682–1686.
12. **Chen, C. S., Y. C. Yao, S. C. Lin, Y. P. Lee, Y. F. Wang, J. R. Wang, C. C. Liu, H. Y. Lei, and C. K. Yu.** 2007. Retrograde axonal transport: a major transmission route of enterovirus 71 in mice. J. Virol. **81**:8996–9003.
13. **Chen, H. F., M. H. Chang, B. L. Chiang, and S. T. Jeng.** 2006. Oral immunization of mice using transgenic tomato fruit expressing VP1 protein from enterovirus 71. Vaccine **24**:2944–2951.
14. **Chen, Y. C., C. K. Yu, Y. F. Wang, C. C. Liu, I. J. Su, and H. Y. Lei.** 2004. A murine oral enterovirus 71 infection model with central nervous system involvement. J. Gen. Virol. **85**:69–77.
15. **Chiu, C. H., C. Chu, C. C. He, and T. Y. Lin.** 2006. Protection of neonatal mice from lethal enterovirus 71 infection by maternal immunization with attenuated Salmonella enterica serovar Typhimurium expressing VP1 of enterovirus 71. Microbes Infect. **8**:1671–1678.
16. **Chumakov, M., M. Voroshilova, L. Shindarov, I. Lavrova, L. Gracheva, G. Koroleva, S. Vasilenko, I. Brodvarova, M. Nikolova, S. Gyurova, M.**

Gacheva, G. Mitov, N. Ninov, E. Tsylka, I. Robinson, M. Frolova, V. Bashkirtsev, L. Martiyanova, and V. Rodin. 1979. Enterovirus 71 isolated from cases of epidemic poliomyelitis-like disease in Bulgaria. Arch. Virol. 60:329–340.
17. Couderc, T., F. Delpeyroux, H. Le Blay, and B. Blondel. 1996. Mouse adaptation determinants of poliovirus type 1 enhance viral uncoating. J. Virol. 70:305–312.
18. Graham, F. L., J. Smiley, W. C. Russell, and R. Nairn. 1977. Characteristics of a human cell line transformed by DNA from human adenovirus type 5. J. Gen. Virol. 36:59–74.
19. Hagiwara, A., I. Tagaya, and T. Yoneyama. 1978. Epidemic of hand, foot and mouth disease associated with enterovirus 71 infection. Intervirology 9: 60–63.
20. Harvala, H., H. Kalimo, J. Bergelson, G. Stanway, and T. Hyypia. 2005. Tissue tropism of recombinant coxsackieviruses in an adult mouse model. J. Gen. Virol. 86:1897–1907.
21. Hashimoto, I., and A. Hagiwara. 1983. Comparative studies on the neurovirulence of temperature-sensitive and temperature-resistant viruses of enterovirus 71 in monkeys. Acta Neuropathol. (Berlin) 60:266–270.
22. Hashimoto, I., and A. Hagiwara. 1982. Pathogenicity of a poliomyelitis-like disease in monkeys infected orally with enterovirus 71: a model for human infection. Neuropathol. Appl. Neurobiol. 8:149–156.
23. Ho, M., E. R. Chen, K. H. Hsu, S. J. Twu, K. T. Chen, S. F. Tsai, J. R. Wang, and S. R. Shih. 1999. An epidemic of enterovirus 71 infection in Taiwan. N. Engl. J. Med. 341:929–935.
24. Horie, H., S. Koike, T. Kurata, Y. Sato-Yoshida, I. Ise, Y. Ota, S. Abe, K. Hioki, H. Kato, C. Taya, T. Nomura, S. Hashizume, H. Yonekawa, and A. Nomoto. 1994. Transgenic mice carrying the human poliovirus receptor: new animal models for study of poliovirus neurovirulence. J. Virol. 68:681–688.
25. Huang, C. C., C. C. Liu, Y. C. Chang, C. Y. Chen, S. T. Wang, and T. F. Yeh. 1999. Neurologic complications in children with enterovirus 71 infection. N. Engl. J. Med. 341:936–942.
26. Ida-Hosonuma, M., T. Iwasaki, T. Yoshikawa, N. Nagata, Y. Sato, T. Sata, M. Yoneyama, T. Fujita, C. Taya, H. Yonekawa, and S. Koike. 2005. The alpha/beta interferon response controls tissue tropism and pathogenicity of poliovirus. J. Virol. 79:4460–4469.
27. Jackson, C. A., C. Cobbs, J. D. Peduzzi, M. Novak, and C. D. Morrow. 2001. Repetitive intrathecal injections of poliovirus replicons result in gene expression in neurons of the central nervous system without pathogenesis. Hum. Gene Ther. 12:1827–1841.
28. Karber, G. 1931. Beitrag zur kollektiven Behandlung pharmakologischer Reihenversuche. Arch. Exp. Pathol. Pharm. 162:480.
29. Kataoka, S., J. Satoh, H. Fujiya, T. Toyota, R. Suzuki, K. Itoh, and K. Kumagai. 1983. Immunologic aspects of the nonobese diabetic (NOD) mouse. Abnormalities of cellular immunity. Diabetes 32:247–253.
30. Kauder, S. E., and V. R. Racaniello. 2004. Poliovirus tropism and attenuation are determined after internal ribosome entry. J. Clin. Investig. 113:1743–1753.
31. Kawamura, N., M. Kohara, S. Abe, T. Komatsu, K. Tago, M. Arita, and A. Nomoto. 1989. Determinants in the 5′ noncoding region of poliovirus Sabin 1 RNA that influence the attenuation phenotype. J. Virol. 63:1302–1309.
32. Kew, O. M., R. W. Sutter, E. M. de Gourville, W. R. Dowdle, and M. A. Pallansch. 2005. Vaccine-derived polioviruses and the endgame strategy for global polio eradication. Annu. Rev. Microbiol. 59:587–635.
33. Kirchgessner, C. U., C. K. Patil, J. W. Evans, C. A. Cuomo, L. M. Fried, T. Carter, M. A. Oettinger, and J. M. Brown. 1995. DNA-dependent kinase (p350) as a candidate gene for the murine SCID defect. Science 267:1178–1183.
34. Koike, S., H. Horie, I. Ise, A. Okitsu, M. Yoshida, N. Iizuka, K. Takeuchi, T. Takegami, and A. Nomoto. 1990. The poliovirus receptor protein is produced both as membrane-bound and secreted forms. EMBO J. 9:3217–3224.
35. Koike, S., C. Taya, T. Kurata, S. Abe, I. Ise, H. Yonekawa, and A. Nomoto. 1991. Transgenic mice susceptible to poliovirus. Proc. Natl. Acad. Sci. USA 88:951–955.
36. Komatsu, H., Y. Shimizu, Y. Takeuchi, H. Ishiko, and H. Takada. 1999. Outbreak of severe neurologic involvement associated with enterovirus 71 infection. Pediatr. Neurol. 20:17–23.
37. La Monica, N., J. W. Almond, and V. R. Racaniello. 1987. A mouse model for poliovirus neurovirulence identifies mutations that attenuate the virus for humans. J. Virol. 61:2917–2920.
38. Liu, C. C., W. C. Lian, M. Butler, and S. C. Wu. 2007. High immunogenic enterovirus 71 strain and its production using serum-free microcarrier Vero cell culture. Vaccine 25:19–24.
39. Liu, M. L., Y. P. Lee, Y. F. Wang, H. Y. Lei, C. C. Liu, S. M. Wang, I. J. Su, J. R. Wang, T. M. Yeh, S. H. Chen, and C. K. Yu. 2005. Type I interferons protect mice against enterovirus 71 infection. J. Gen. Virol. 86:3263–3269.
40. Lum, L. C., K. T. Wong, S. K. Lam, K. B. Chua, A. Y. Goh, W. L. Lim, B. B. Ong, G. Paul, S. AbuBakar, and M. Lambert. 1998. Fatal enterovirus 71 encephalomyelitis. J. Pediatr. 133:795–798.
41. Martin, A., D. Benichou, T. Couderc, J. M. Hogle, C. Wychowski, S. Van der Werf, and M. Girard. 1991. Use of type 1/type 2 chimeric polioviruses to study determinants of poliovirus type 1 neurovirulence in a mouse model. Virology 180:648–658.
42. Martin, A., C. Wychowski, T. Couderc, R. Crainic, J. Hogle, and M. Girard. 1988. Engineering a poliovirus type 2 antigenic site on a type 1 capsid results in a chimaeric virus which is neurovirulent for mice. EMBO J. 7:2839–2847.
43. McGoldrick, A., A. J. Macadam, G. Dunn, A. Rowe, J. Burlison, P. D. Minor, J. Meredith, D. J. Evans, and J. W. Almond. 1995. Role of mutations G-480 and C-6203 in the attenuation phenotype of Sabin type 1 poliovirus. J. Virol. 69:7601–7605.
44. McMinn, P. C. 2002. An overview of the evolution of enterovirus 71 and its clinical and public health significance. FEMS Microbiol. Rev. 26:91–107.
45. Mendelsohn, C. L., E. Wimmer, and V. R. Racaniello. 1989. Cellular receptor for poliovirus: molecular cloning, nucleotide sequence, and expression of a new member of the immunoglobulin superfamily. Cell 56:855–865.
46. Minor, P. D. 1992. The molecular biology of polio vaccines. J. Gen. Virol. 73:3065–3077.
47. Murray, M. G., J. Bradley, X. F. Yang, E. Wimmer, E. G. Moss, and V. R. Racaniello. 1988. Poliovirus host range is determined by a short amino acid sequence in neutralization antigenic site I. Science 241:213–215.
48. Nagata, N., T. Iwasaki, Y. Ami, A. Harashima, I. Hatano, Y. Suzaki, K. Yoshii, T. Yoshii, A. Nomoto, and T. Kurata. 2001. Comparison of neuropathogenicity of poliovirus type 3 in transgenic mice bearing the poliovirus receptor gene and cynomolgus monkeys. Vaccine 19:3201–3208.
49. Nagata, N., T. Iwasaki, Y. Ami, Y. Tano, A. Harashima, Y. Suzaki, Y. Sato, H. Hasegawa, T. Sata, T. Miyamura, and H. Shimizu. 2004. Differential localization of neurons susceptible to enterovirus 71 and poliovirus type 1 in the central nervous system of cynomolgus monkeys after intravenous inoculation. J. Gen. Virol. 85:2981–2989.
50. Nagata, N., H. Shimizu, Y. Ami, Y. Tano, A. Harashima, Y. Suzaki, Y. Sato, T. Miyamura, T. Sata, and T. Iwasaki. 2002. Pyramidal and extrapyramidal involvement in experimental infection of cynomolgus monkeys with enterovirus 71. J. Med. Virol. 67:207–216.
51. Nijhuis, M., N. van Maarseveen, R. Schuurman, S. Verkuijlen, M. de Vos, K. Hendriksen, and A. M. van Loon. 2002. Rapid and sensitive routine detection of all members of the genus enterovirus in different clinical specimens by real-time PCR. J. Clin. Microbiol. 40:3666–3670.
52. Omata, T., M. Kohara, S. Kuge, T. Komatsu, S. Abe, B. L. Semler, A. Kameda, H. Itoh, M. Arita, E. Wimmer, and A. Nomoto. 1986. Genetic analysis of the attenuation phenotype of poliovirus type 1. J. Virol. 58:348–358.
53. Paul, A. V., J. Mugavero, J. Yin, S. Hobson, S. Schultz, J. H. van Boom, and E. Wimmer. 2000. Studies on the attenuation phenotype of polio vaccines: poliovirus RNA polymerase derived from Sabin type 1 sequence is temperature sensitive in the uridylylation of VPg. Virology 272:72–84.
54. Pulli, T., P. Koskimies, and T. Hyypia. 1995. Molecular comparison of coxsackie A virus serotypes. Virology 212:30–38.
55. Ren, R. B., F. Costantini, E. J. Gorgacz, J. J. Lee, and V. R. Racaniello. 1990. Transgenic mice expressing a human poliovirus receptor: a new model for poliomyelitis. Cell 63:353–362.
56. Ren, R. B., E. G. Moss, and V. R. Racaniello. 1991. Identification of two determinants that attenuate vaccine-related type 2 poliovirus. J. Virol. 65: 1377–1382.
57. Rezapkin, G. V., L. Fan, D. M. Asher, M. R. Fibi, E. M. Dragunsky, and K. M. Chumakov. 1999. Mutations in Sabin 2 strain of poliovirus and stability of attenuation phenotype. Virology 258:152–160.
58. Sabin, A. B. 1965. Oral poliovirus vaccine. History of its development and prospects for eradication of poliomyelitis. JAMA 194:872–876.
59. Sambrook, J., and D. W. Russell. 2001. Molecular cloning: a laboratory manual, 3rd ed., p 13.19–13.25. Cold Spring Harbor Laboratory Press, Cold Spring Harbor, NY.
60. Schmidt, N. J., E. H. Lennette, and H. H. Ho. 1974. An apparently new enterovirus isolated from patients with disease of the central nervous system. J. Infect. Dis. 129:304–309.
61. Shih, S. R., M. C. Tsai, S. N. Tseng, K. F. Won, K. S. Shia, W. T. Li, J. H. Chern, G. W. Chen, C. C. Lee, Y. C. Lee, K. C. Peng, and Y. S. Chao. 2004. Mutation in enterovirus 71 capsid protein VP1 confers resistance to the inhibitory effects of pyridyl imidazolidinone. Antimicrob. Agents Chemother. 48:3523–3529.
62. Shiroki, K., T. Ishii, T. Aoki, Y. Ota, W. X. Yang, T. Komatsu, Y. Ami, M. Arita, S. Abe, S. Hashizume, and A. Nomoto. 1997. Host range phenotype induced by mutations in the internal ribosomal entry site of poliovirus RNA. J. Virol. 71:1–8.
63. Smyth, M., J. Tate, E. Hoey, C. Lyons, S. Martin, and D. Stuart. 1995. Implications for viral uncoating from the structure of bovine enterovirus. Nat. Struct. Biol. 2:224–231.
64. Tan, C. S., and M. J. Cardosa. 2007. High-titred neutralizing antibodies to human enterovirus 71 preferentially bind to the N-terminal portion of the capsid protein VP1. Arch. Virol. 152:1069–1073.
65. Tardy-Panit, M., B. Blondel, A. Martin, F. Tekaia, F. Horaud, and F. Delpeyroux. 1993. A mutation in the RNA polymerase of poliovirus type 1 contributes to attenuation in mice. J. Virol. 67:4630–4638.
66. Tung, W. S., S. A. Bakar, Z. Sekawi, and R. Rosli. 2007. DNA vaccine

constructs against enterovirus 71 elicit immune response in mice. Genet. Vaccines Ther. 5:6.
67. **Utagawa, E. T., E. Nakazawa, K. Matsuo, I. Oishi, N. Takeda, and T. Miyamura.** 2002. Application of an automated specimen search system installed in a transmission electron microscope for the detection of caliciviruses in clinical specimens. J. Virol. Methods **100**:49–56.
68. **Wagner-Ballon, O., H. Chagraoui, E. Prina, M. Tulliez, G. Milon, H. Raslova, J. L. Villeval, W. Vainchenker, and S. Giraudier.** 2006. Monocyte/macrophage dysfunctions do not impair the promotion of myelofibrosis by high levels of thrombopoietin. J. Immunol. **176**:6425–6433.
69. **Wang, S. M., H. Y. Lei, K. J. Huang, J. M. Wu, J. R. Wang, C. K. Yu, I. J. Su, and C. C. Liu.** 2003. Pathogenesis of enterovirus 71 brainstem encephalitis in pediatric patients: roles of cytokines and cellular immune activation in patients with pulmonary edema. J. Infect. Dis. **188**:564–570.
70. **Wang, S. M., C. C. Liu, H. W. Tseng, J. R. Wang, C. C. Huang, Y. J. Chen, Y. J. Yang, S. J. Lin, and T. F. Yeh.** 1999. Clinical spectrum of enterovirus 71 infection in children in southern Taiwan, with an emphasis on neurological complications. Clin. Infect. Dis. **29**:184–190.
71. **Wang, Y. F., C. T. Chou, H. Y. Lei, C. C. Liu, S. M. Wang, J. J. Yan, I. J. Su, J. R. Wang, T. M. Yeh, S. H. Chen, and C. K. Yu.** 2004. A mouse-adapted enterovirus 71 strain causes neurological disease in mice after oral infection. J. Virol. **78**:7916–7924.
72. **Wu, T. C., Y. F. Wang, Y. P. Lee, J. R. Wang, C. C. Liu, S. M. Wang, H. Y. Lei, I. J. Su, and C. K. Yu.** 2007. Immunity to avirulent enterovirus 71 and coxsackie A16 virus protect against enterovirus 71 infection in mice. J. Virol. **81**:10310–10315.
73. **Yu, C. K., C. C. Chen, C. L. Chen, J. R. Wang, C. C. Liu, J. J. Yan, and I. J. Su.** 2000. Neutralizing antibody provided protection against enterovirus type 71 lethal challenge in neonatal mice. J. Biomed. Sci. **7**:523–528.

Journal of General Virology (2008), 89, 2518–2530 DOI 10.1099/vir.0.2008/002915-0

Characterization of pharmacologically active compounds that inhibit poliovirus and enterovirus 71 infectivity

Minetaro Arita, Takaji Wakita and Hiroyuki Shimizu

Correspondence
Minetaro Arita
minetaro@nih.go.jp

Department of Virology II, National Institute of Infectious Diseases, 4-7-1 Gakuen, Musashimurayama-shi, Tokyo 208-0011, Japan

Poliovirus (PV) and enterovirus 71 (EV71) cause severe neurological symptoms in their infections of the central nervous system. To identify compounds with anti-PV and anti-EV71 activities that would not allow the emergence of resistant mutants, we performed drug screening by utilizing a pharmacologically active compound library targeting cellular factors with PV and EV71 pseudoviruses that encapsidated luciferase-encoding replicons. We have found that metrifudil (*N*-[2-methylphenyl]methyl)-adenosine) (an A2 adenosine receptor agonist), N^6-benzyladenosine (an A1 adenosine receptor agonist) and NF449 (4,4′,4″,4‴-[carbonylbis[imino-5,1,3-benzenetriyl bis(carbonyl-imino)]] tetrakis (benzene-1,3-disulfonic acid) octasodium salt) (a Gs-α inhibitor) have anti-EV71 activity, and that GW5074 (3-(3, 5-dibromo-4-hydroxybenzylidine-5-iodo-1,3-dihydro-indol-2-one)) (a Raf-1 inhibitor) has both anti-PV and anti-EV71 activities. EV71 mutants resistant to metrifudil, N^6-benzyladenosine and NF449 were isolated after passages in the presence of these compounds, but mutants resistant to GW5074 were not isolated for both PV and EV71. The inhibitory effect of GW5074 was not observed in Sendai virus infection and the treatment did not induce the expression of OAS1 and STAT1 mRNA. Small interfering RNA treatment against putative cellular targets of GW5074, including Raf-1, B-Raf, Pim-1, -2, and -3, HIPK2, GAK, MST2 and ATF-3, did not consistently suppress PV replication. Moreover, downregulation of Raf-1 and B-Raf did not affect the sensitivity of RD cells to the inhibitory effect of GW5074. These results suggest that GW5074 has strong and selective inhibitory effect against the replication of PV and EV71 by inhibiting conserved targets in the infection independently of the interferon response.

Received 8 April 2008
Accepted 16 May 2008

INTRODUCTION

Poliovirus (PV) is a small, non-enveloped virus with a single-stranded positive genomic RNA of about 7500 nt, belonging to the genus *Enterovirus* of the family *Picornaviridae*. PV is the causative agent of poliomyelitis, where the motor neurones are the major target (Bodian, 1949). The tropism of PV to the motor neurones is attributable in part to the expression of the PV receptor (PVR) (Crotty *et al.*, 2002; Ida-Hosonuma *et al.*, 2002; Koike *et al.*, 1994; Ren & Racaniello, 1992). Enterovirus 71 (EV71) belongs to the genus *Enterovirus* but was classified into a different species from PV, *Human enterovirus species A*. EV71 is a causative agent of hand, foot and mouth disease and herpangina, but sometimes causes severe neurological diseases, such as brainstem encephalitis and poliomyelitis-like paralysis (Chumakov *et al.*, 1979; McMinn, 2002; Wang *et al.*, 2003). The case-severity rate of EV71 in an outbreak in Taiwan was <0.3% (Ho *et al.*, 1999), suggesting a high neuropathogenicity of EV71 as well as PV, which causes poliomyelitis in 0.1–1.0% of infected individuals (reviewed by Minor, 1992). EV71 causes fatal pulmonary oedema and/or pulmonary haemorrhage in young children by destruction of the vasomotor and respiratory centres in the brain stem (Chang *et al.*, 1999; Ho *et al.*, 1999; Huang *et al.*, 1999; Komatsu *et al.*, 1999; Lum *et al.*, 1998; Wang *et al.*, 1999).

The viral replication machinery of PV requires numerous cellular factors to hijack the cellular process. For viral protein synthesis, recruitment of ribosome to the internal ribosomal entry site (IRES) on the viral genome requires host factors polypyrimidine tract-binding protein (PTB), Unr, La, poly(rC)-binding protein 2 (PCBP2) and SRp20 that are not required for cap-dependent protein synthesis of cellular mRNA (Bedard *et al.*, 2007; Hellen *et al.*, 1993; Hunt *et al.*, 1999; Meerovitch *et al.*, 1993; Sanford *et al.*, 2004; Walter *et al.*, 1999), along with proteolytic modification of a translation initiation factor eIF4G by viral proteinase $2A^{pro}$ to hijack the translation machinery from

A supplementary table showing the siRNA duplex used in this study is available with the online version of this paper.

cap-dependent protein synthesis to viral protein synthesis (Gradi *et al.*, 1998; Krausslich *et al.*, 1987). For the replication process, membrane rearrangement utilizing ADP ribosylation factors (Arfs) and guanine nucleotide exchange factors (GEFs) (GBF1, BIG1/2) are required via direct and indirect interaction with viral 3A and 3CD proteins in coxsackievirus B3 (CVB3) and PV infections (Belov *et al.*, 2007; Wessels *et al.*, 2006). Cellular signalling via extracellular signal-regulated kinase (ERK), phosphatidylinositol 3-kinase (PI3K) and stress-activated protein kinases (SAPKs) affected replication and/or the release of progeny virus in CVB3 infection by an unknown mechanism (Esfandiarei *et al.*, 2004; Luo *et al.*, 2002; Si *et al.*, 2005).

These cellular processes are promising targets for the development of effective anti-PV drugs. PV mutants resistant to anti-PV inhibitors or anti-PV antibodies could emerge rapidly, because a mutant exists in a population of virus (10^3 to 10^5), if a single mutation was sufficient for resistance (Blondel *et al.*, 1986; Crotty *et al.*, 2001; de la Torre *et al.*, 1992; Diamond *et al.*, 1985; Pincus *et al.*, 1986, 1987). Actually, PV isolates from an immunodeficient case chronically infected with PV showed resistance to pleconaril, which is an anti-PV drug that targets the viral capsid proteins to prevent uncoating (Abdel-Rahman & Kearns, 1998), despite the absence of pleconaril treatment (MacLennan *et al.*, 2004). In contrast, emergence of virus mutant resistant to inhibitors against cellular factors was limited, depending in part on the capacity of viral protein activities in the target step. A PV mutant resistant to brefeldin A, which blocks membrane traffic between the *cis*- and *trans*-Golgi compartments and inhibits PV replication (Irurzun *et al.*, 1992; Maynell *et al.*, 1992), required two mutations and was isolated after five passages under a stepwise selection pressure by raising the concentration of the inhibitor (Crotty *et al.*, 2004). The emergence of a PV mutant resistant to geldanamycin treatment, which targets Hsp90 and interferes with the folding of PV capsid probably in cooperation with Hsp70 (Macejak & Sarnow, 1992), was not observed (Geller *et al.*, 2007).

In this study, we performed drug screening by utilizing a pharmacologically active compound library with partially characterized targets and pseudoviruses, which have PV and EV71 replicons encoding firefly luciferase as a replication marker encapsidated in the PV and EV71 capsid proteins, respectively (Arita *et al.*, 2006, 2008, Porter *et al.*, 1998). We have identified four compounds and characterized their inhibitory effects on PV and EV71 infection.

METHODS

Cells, viruses, reagents and drug library. HEK293 cells (human embryonic kidney cell line) (Graham *et al.*, 1977), RD cells (human rhabdomyosarcoma cell line), HEp-2c (human larynx epidermoid carcinoma cell line) and L20B cells (mouse Ltk$^-$aprt$^-$ fibroblast cell line expressing PV receptor) (Mendelsohn *et al.*, 1989) were cultured as monolayers in Dulbecco's modified Eagle medium (DMEM) supplemented with 10% fetal calf serum (FCS). HEK293 cells were used for preparation of pseudoviruses. RD cells were used for titration of pseudoviruses and for drug screening. PV and EV71 pseudoviruses, which encapsidated luciferase-encoding PV and EV71 replicons with capsid proteins derived from PV (Mahoney) and EV71 (Nagoya), respectively, were prepared as reported previously (Arita *et al.*, 2006, 2008), except that the *Eco*RI site in the 5′NTR of PV replicon was removed by site-directed mutagenesis. A Sendai virus (SeV) mutant (SeV/luc), which encodes luciferase (Hasan *et al.*, 1997), was a generous gift from Atsushi Kato, Department of Virology III, National Institute of Infectious Diseases, Tokyo, Japan. N^6-Benzyladenosine (Acros Organics), SL 327 (Sigma-Aldrich) and U0126 (Sigma-Aldrich) were dissolved in DMSO to prepare a 10 mM solution, and this was diluted with 10% FCS/DMEM to prepare a 0.5 mM solution before use. LOPAC^{1280} drug library (Sigma-Aldrich) was used for drug screening. Each drug (10 mM solution in DMSO) was diluted with 10% FCS/DMEM to 0.5 mM before use.

Virus titration. The virus titre was determined by measuring 50% cell culture infectious dose ($CCID_{50}$) in a microtitration assay using RD cells, as described elsewhere (Nagata *et al.*, 2002). Briefly, inoculated RD cells were cultured at 37 °C for 7 days, and were then observed for cytopathic effects (CPE). $CCID_{50}$ was calculated using the Behrens–Kärber method (Kärber, 1931).

Drug screening. RD cells (1.0×10^4 cells per well in 100 µl medium) were cultured at 37 °C in 96-well plates (White Opaque Tissue Culture Plate; Becton Dickinson), followed by addition of 10 µl of 0.5 mM drug solution (final concentration of 45 µM). The cells were incubated at 37 °C for 0 or 48 h. The cells were inoculated with 100 infectious units (IU) of PV or EV71 pseudovirus in 50 µl of 10% FCS/DMEM, and then were incubated at 37 °C for 9 h (the final concentration of drugs was 31 µM). Luciferase activity of the cells was measured with Luciferase Assay System (Promega) using a TR717 Microplate luminometer (ABI) according to the manufacturer's instructions. The inhibition index, which is the ratio of luciferase activity in the drug-treated cells to that in mock-treated cells (1.0 for mock-treated cells), was determined for each drug. 50% inhibitory concentration (IC_{50}), at which the drugs suppressed the infection of pseudovirus by 50% at 9 h post-inoculation (p.i.), was determined for the drugs that showed either anti-PV or anti-EV71 activity.

Evaluation of cytotoxicity of drugs. Cytotoxicity of drugs was evaluated by two methods: observation of cell viability at 3 days after drug treatment under the same condition as for the screening (described above) and determination of the 50% cytotoxic concentration (CC_{50}) of drugs by the measurement of ATP as a marker of metabolically active cells. For the measurement of ATP in cells, RD cells (3.8×10^4 cells per well in 100 µl medium) were cultured at 37 °C in 96-well plates (Becton Dickinson), followed by addition of 10 µl of drug solution. The ranges of the concentration of drugs examined were as follows: GW5074, 0.13–0.5 mM; metrifudil, 0.0063–0.05 mM; N^6-benzyladenosine, 1.3–10 mM; NF449, 0.13–1.0 mM. The cells were incubated at 37 °C for 9 h, and were then subjected to the measurement of ATP by using a CellTiter-Glo Luminescent Cell Viability Assay kit (Promega) according to the manufacturer's instructions.

Measurement of anti-PV and anti-EV71 activities of inhibitors. Virus solution (containing 10^5 $CCID_{50}$ in 5 µl 10% FCS/DMEM) was added to RD cells (2.8×10^4 cells per well in 100 µl 10% FCS/DMEM) in 96-well plates (Becton Dickinson), and then the cells were incubated at 37 °C for 2 h. The cells were washed three times with 10% FCS/DMEM, followed by the addition of 100 µl of 10% FCS/DMEM containing each inhibitor or without the inhibitor as control.

The concentrations of inhibitors examined were: 50 μM GW5074, 25 μM metrifudil, 2.5 μM N^6-benzyladenosine and 50 μM NF449. The cells were then incubated at 37 °C for 7 h and collected at 9 h p.i. and stored at −70 °C. For the analysis of the effect of NF449 on virus adsorption and/or uncoating, the inhibitor was added to the cells just before adding the virus solution, and the cells were then incubated at 37 °C for 2 h, followed by three washes with 10% FCS/DMEM and incubated in the absence of NF449 at 37 °C for 7 h (0–2 h incubation, Table 2). The viral RNA was extracted from the collected cells using a High Pure Viral RNA purification kit (Roche), and the number of copies of viral RNA was quantified using a real-time TaqMan PCR system (described below). The inhibition index, which is the ratio of the luciferase activity or of the number of copies of viral RNA in inhibitor-treated cells to that in mock-treated cells (1.0 for mock-treated cells), was determined for each inhibitor (Fig. 2 and Table 2).

Quantification of viral RNA by real-time TaqMan PCR. Real-time TaqMan PCR was performed as previously described by Nijhuis *et al.* (2002). Isolated viral RNA was reverse transcribed using a Reverse Transcription System (Promega) with random hexamers according to the manufacturer's instructions. The resultant cDNA was assayed in a 20 μl reaction mixture containing 2 μl cDNA solution, 10 μl TaqMan Fast Universal PCR Master Mix (Applied Biosystems) with primers (Forward primer and Reverse primer 1) and probe (Probe 1) (Nijhuis *et al.*, 2002). Plasmid DNA of an EV71 infectious clone [pEV71(Nagoya)] was used as the control for quantification of the number of copies (Arita *et al.*, 2007). The mixtures were subjected to real-time PCR; PCR conditions were: denaturation step at 95 °C for 20 s and 40 cycles of thermal cycling at 95 °C for 3 s and 60 °C for 30 s. The fluorescence emission of the probe was monitored and analysed by using an Applied Biosystems 7500 Fast Real-Time PCR System (Applied Biosystems).

Isolation of PV and EV71 mutants resistant to inhibitors. Virus solutions of PV1(Mahoney), EV71(BrCr-TR) and EV71(Nagoya) (containing 10^6 $CCID_{50}$ in 5 μl 10% FCS/DMEM) were added to RD cells (1.0×10^4 cells per well in 100 μl 10% FCS/DMEM) in 96-well plates (Becton Dickinson) in the presence of the inhibitors. The concentrations of inhibitors examined were: 25–100 μM GW5074, 10 μM metrifudil, 0.25–5 μM N^6-benzyladenosine and 25–100 μM NF449. The cells were incubated at 37 °C and collected when all the cells exhibited CPE or at day 3 p.i. Collected cell lysates for each inhibitor were mixed and then used for the next passage in the presence of each inhibitor. The passage was repeated twelve times or until a resistant phenotype was observed for the isolates compared with the parental strains in the presence of each inhibitor. The viral RNAs of the isolates were extracted from the collected cell lysates by using a High Pure Viral RNA purification kit (Roche), and the sequences of the viral genomes of the isolates were analysed in the capsid protein coding region (for mutant resistant to NF449) or in the non-structural protein coding region (for mutants resistant to metrifudil and N^6-benzyladenosine) to identify the mutations required for the resistance.

Knockdown analysis by RNA interference (RNAi). Knockdown analysis was performed by utilizing RNAi with small interfering RNA (siRNA; Elbashir *et al.*, 2001). Three sets of siRNA against Raf-1, B-Raf, Pim-1, -2 and -3, HIPK2, GAK, MST2 and ATF-3 were designed in the conserved regions among the transcript variants and were prepared as 50 μM solutions of RNA duplex (Supplementary Table S1). For negative controls of each siRNA, RNA duplex with scramble sequences against each cellular-mRNA-specific RNA duplex, which did not show specificity to known cellular mRNAs but with the same nucleotide constitution as the cellular-mRNA-specific RNA duplex, was designed and prepared as 50 μM solutions of RNA duplex. RNA duplex solution (final concentration 0.1 μM) was transfected into RD cells (8.0×10^3 cells) in 96-well plates by using Lipofectamine RNAiMAX Reagent (Invitrogen) according to the manufacturer's instructions. The cells were incubated at 37 °C for 48 h and the supernatant was removed and replaced with 100 μl per well of 10% FCS/DMEM. At 72 h post-transfection, the cells were inoculated with 100 IU PV pseudovirus in 100 μl 10% FCS/DMEM, and then were incubated at 37 °C for 8 h. Luciferase activity in the cells was measured with the Luciferase Assay System (Promega) using TR717 Microplate luminometer (ABI) according to the manufacturer's instructions. For Western blot analysis of Raf-1 and B-Raf, RNA duplex solution (final concentration 0.1 μM) was transfected into RD cells (2.0×10^5 cells) in 6-well plates by using Lipofectamine RNAiMAX Reagent (Invitrogen) according to the manufacturer's instructions. The cells were incubated at 37 °C for 48 h and the supernatant was removed and replaced with 2 ml 10% FCS/DMEM per well. The cells were further incubated at 37 °C for 24 h, and were then subjected to Western blot analysis.

Western blot analysis. siRNA-treated RD cells (3.9×10^5 cells) were collected in 100 μl cell lysis buffer [21 mM HEPES buffer (pH 7.4), 1.8 mM disodium hydrogenphosphate, 137 mM NaCl, 4.8 mM KCl, 0.5% Nonidet P-40 and 0.5 mM EDTA] at 72 h post-transfection, and then were subjected to 5–20% gradient PAGE (e-PAGEL; Atto) in a Laemmli buffer system (Laemmli, 1970). The proteins in the gel were transferred to a polyvinylidene difluoride filter (Immobilon; Millipore) and blocked in phosphate-buffered saline (PBS) [10 mM phosphate buffer (pH 7.0), 135 mM NaCl and 2.6 mM KCl] containing 5% non-fat dry milk. The filters were incubated with rabbit anti-Raf-1 antibody (Sigma) or with anti-B-Raf antibody (Santa Cruz Biotechnology) (1 : 500 and 1 : 50 dilution in PBS containing 0.1% Tween 20 and 0.5% non-fat dry milk, respectively) at room temperature for 1 h. The filters were washed with PBS containing 0.1% Tween 20 three times for 5 min each, and then incubated with donkey anti-rabbit IgG antibodies conjugated with horseradish peroxidase (Amersham Biosciences) (1 : 1000 dilution in PBS containing 0.1% Tween 20 and 0.5% non-fat dry milk) at room temperature for 1 h. The filters were washed with PBS containing 0.1% Tween 20 three times for 5 min each, and then treated with SuperSignal West Femto Maximum Sensitivity Substrate (Pierce Biotechnology) for the detection of the signal.

Measurement of the interferon response. RD cells (2.8×10^5 cells) in 6-well plates were treated with siRNA (for Raf-1 and B-Raf, collected at 72 h post-transfection), GW5074 (6.25 μM or 25 μM at 37 °C, collected after 4 h incubation) or poly IC (collected at 24 h post-transfection), and the total RNA was extracted from the treated cells with a High Pure RNA Isolation kit (Roche). The relative expression levels of OAS1 and STAT1 mRNAs in the cells were determined by real-time PCR using primers in an IFN Response Watcher kit (TaKaRa) with a One Step SYBR PrimeScript RT-PCR kit II (Perfect Real Time) kit (TaKaRa). β-actin mRNA was used as the endogenous control, and the expression levels of OAS1 and STAT1 mRNAs in treated cells were normalized by the expression levels in the mock-treated cells.

RESULTS

Strategy of drug screening for anti-enterovirus drugs

To identify anti-PV and anti-EV71 drugs, we screened the LOPAC^{1280} drug library. We utilized PV and EV71 pseudoviruses that have PV and EV71 capsid protein-encapsidated luciferase-encoding PV and EV71 replicons,

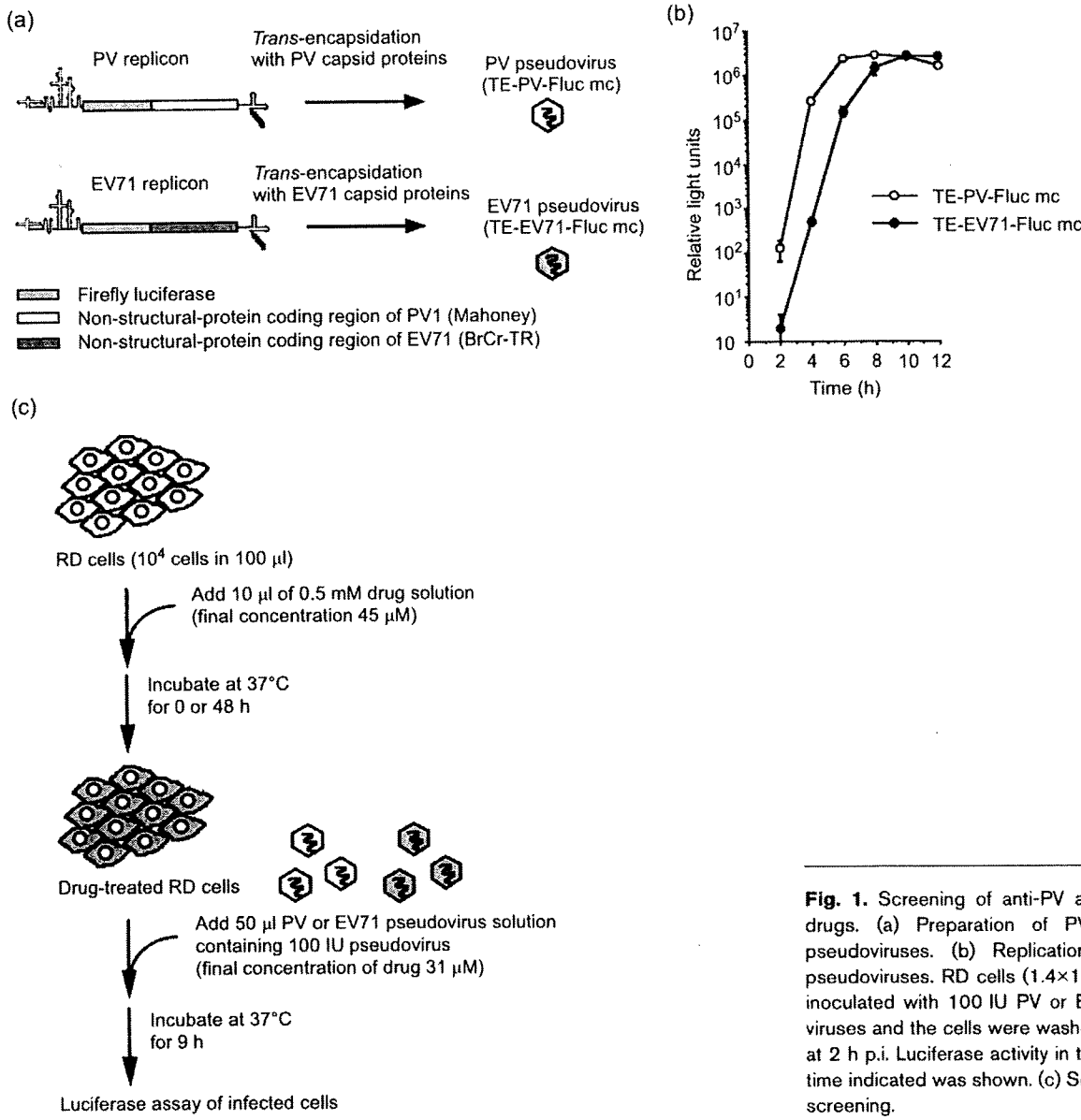

Fig. 1. Screening of anti-PV and anti-EV71 drugs. (a) Preparation of PV and EV71 pseudoviruses. (b) Replication kinetics of pseudoviruses. RD cells (1.4×10^4 cells) were inoculated with 100 IU PV or EV71 pseudoviruses and the cells were washed three times at 2 h p.i. Luciferase activity in the cells at the time indicated was shown. (c) Scheme of drug screening.

respectively (Fig. 1a). Both the short and long-term effects of the compounds were examined by preincubating RD cells with compounds for 0 and 48 h before pseudovirus infection, respectively (Fig. 1c). We defined anti-enterovirus activity of the compounds as suppression of luciferase activity in the treated cells by less than 10^{-4}-fold of that observed in mock-treated cells beyond the deviation of false-positive decline in luciferase signals caused by the drug treatment. The mean relative light units in mock-treated cells inoculated with PV and EV71 pseudoviruses (obtained from 16 wells of each plate) were 1.7×10^7 (with a standard deviation of 1.2×10^6) and 4.5×10^6 (with a standard deviation of 7.2×10^5), respectively.

Identification of anti-PV and anti-EV71 inhibitors

In the screening, we identified a total of 101 compounds that reduced either PV or EV71 pseudovirus infectivity. We examined the cytotoxicity of these compounds and found that most of them had strong cytotoxicity at the concentration examined, leaving substantially no viable cells after the treatment (Fig. 2b, toxic effect in the drug-treated cells). However, treatment with three compounds (GW5074, metrifudil and NF449) had apparently no effect on the viability of the cells (Fig. 2a and b). Among these compounds, metrifudil and NF449 specifically inhibited EV71 infection, with inhibition indices of 3.6×10^{-5} and 2.6×10^{-4}, respectively. In contrast, GW5074 inhibited

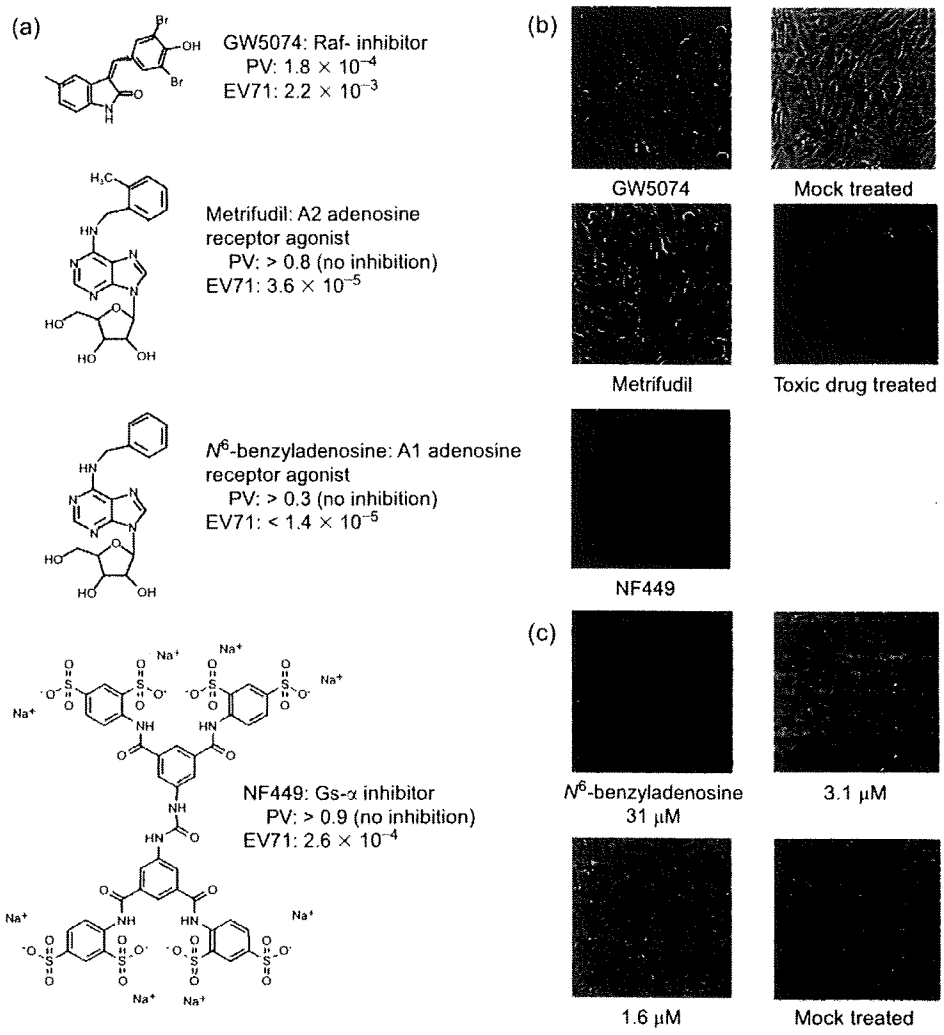

Fig. 2. Idenfication of anti-PV and anti-EV71 inhibitors. (a) Structure of identified inhibitors. The inhibitory effect of each compound against pseudovirus replication is shown as the inhibition index, which was taken as 1.0 in the mock-treated cells (>0.1, no inhibition). (b) Morphology of drug-treated RD cells. RD cells were treated with 31 μM of each compound for 3 days, except NF449 (for 9 h). (c) Morphology of RD cells treated with N^6-benzyladenosine. RD cells were treated with the indicated concentrations of N^6-benzyladenosine for 3 days.

both EV71 and PV infection, with inhibition indices of 2.2×10^{-3} and 1.8×10^{-4}, respectively. Since metrifudil has just become commercially unavailable, we examined adenosine derivatives structurally related to metrifudil for their anti-EV71 activity, and identified N^6-benzyladenosine as a strong anti-EV71 inhibitor (inhibition index of $<1.4 \times 10^{-5}$). Cells treated with GW5074 and N^6-benzyladenosine showed characteristic morphological changes (flattened shape and enlargement of the cell size), in contrast to those treated with metrifudil or NF449. Treatment with N^6-benzyladenosine also affected the viability of the cells at 31 μM, but not at 1.6 μM, after incubation for 3 days (Fig. 2c).

Characterization of identified anti-PV and anti-EV71 inhibitors

We determined the IC_{50} and CC_{50} of identified inhibitors against pseudovirus infection (Fig. 3 and Table 1). The IC_{50} values of the inhibitors against EV71 pseudovirus infection in RD cells were of the micromolar order, except N^6-benzyladenosine, whose IC_{50} was 0.1 μM (Fig. 3a). IC_{50} of GW5074 against PV pseudovirus infection was determined in RD cells and also in cell lines of different origins (HEp-2c and mouse L20B cells). GW5074 was effective in these cells, with an IC_{50} of 2.3–6.0 μM (Fig. 3b). CC_{50} of the inhibitors was determined by measuring ATP derived from

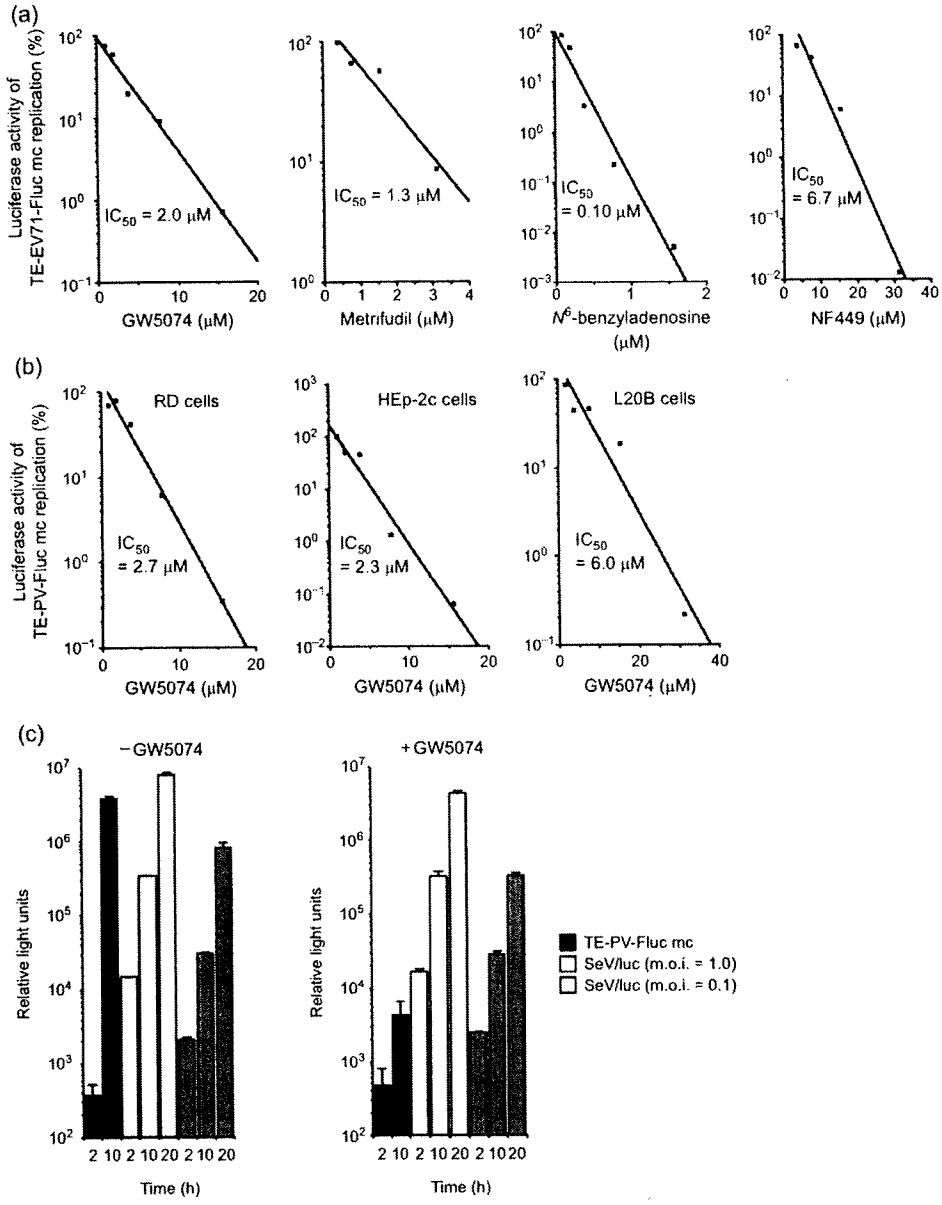

Fig. 3. Characterization of the effect of anti-PV and anti-EV71 inhibitors. (a) Determination of IC_{50} of anti-EV71 inhibitors against EV71 pseudovirus infection in RD cells. (b) Determination of IC_{50} of GW5074 against PV pseudovirus infection in various cell lines. (c) Comparison of the inhibitory effect of GW5074 on PV and SeV infection. RD cells were inoculated with 100 IU PV pseudovirus or with luciferase-encoding SeV (SeV/luc, at a m.o.i. of 1.0 or 0.1) in the presence of GW5074 (31 μM).

viable cells. The selectivity index (SI) of each inhibitor ranged from >38 to 33 000 (Table 1). To examine the specificity of the inhibitory effect of GW5074, we analysed the effect on the infection of SeV, which is a negative strand RNA virus belonging to the family *Paramyxoviridae* (Fig. 3c). GW5074 had no inhibitory effect on SeV infection (at most threefold reduction of luciferase activity in the treated cells), in contrast to its strong inhibitory effect on PV pseudovirus infection.

Next, we analysed the effects of identified inhibitors on the infectivity of PV and EV71 strains (Table 2). As observed for pseudovirus infection, they had strong inhibitory effect on the infectivity of virus strains examined (inhibition indices

Table 1. Properties of identified drugs

Drug	CC_{50} (μM)	IC_{50} for EV71 (μM)	IC_{50} for PV (μM)	SI for EV71	SI for PV	Reversion of EV71	Reversion of PV
Metrifudil	>50	1.3	ND	>38	ND	3 passages (2C)	ND
N^6-benzyladenosine	3300	0.10	ND	33 000	ND	3 passages (2C)	ND
NF449	>1000	6.7	ND	>150	ND	5 passages (VP1)	ND
GW5074	170	2.0	2.7	85	63	No reversion	No reversion

ND, Not determined.

of 10^{-1} to 10^{-5}). The inhibitory effect of GW5074 was the highest against type 3 PV (Sabin) (inhibitory index of 7.0×10^{-5}) and lowest against EV71 (BrCr-TR) (inhibitory index of 1.5×10^{-2}). EV71 (BrCr-TR) also showed partial resistance to NF449 treatment. In this test, metrifudil, N^6-benzyladenosine and NF449 did not show any inhibitory effect on type 1 PV (Sabin) infection. Except for NF449, the inhibitors were effective when added to the inoculated cells after the uncoating step (2 h p.i.). NF449 was effective only when added to the cells during virus infection (0–2 h p.i.), suggesting that NF449 inhibits the adsorption and/or uncoating step of EV71, but not the replication step.

To characterize further the target of these inhibitors, we isolated virus mutants resistant to these inhibitors (Table 1). EV71 mutants resistant to metrifudil, N^6-benzyladenosine and NF449 treatments were isolated within five passages. Sequence analysis of the viral genomes showed mutations in protein 2C in mutants resistant to metrifudil (mutations at nt 5050 and 5815) and to N^6-benzyladenosine (mutations at nt 4428 and 5048), and mutations in VP1 capsid protein were observed in a mutant resistant to NF449 (mutations at nt 2734 and 3173). The critical mutations for the resistant phenotype against each inhibitor were determined by using pseudoviruses carrying corresponding mutations (Fig. 4). The determinants for the resistance to metrifudil, N^6-benzyladenosine and NF449 on the EV71 genome are a single mutation at nt 5050 (change of A to G) resulting in an amino acid change of glutamic acid to glycine at amino acid position 325 of protein 2C for metrifudil resistance, double mutations at nt 4428 and 5048 (changes of C to U and A to G, respectively) resulting in an amino acid changes of histidine to tyrosine and isoleucine to methionine at amino acid positions 118 and 324 of protein 2C for N^6-benzyladenosine resistance, and double mutations at nt 2734 and 3173 (changes of G to C and A to G, respectively) resulting in amino acid changes of glutamic acid to glutamine and lysine to arginine at amino acid positions 98 and 244 of protein VP1 for NF449 resistance. In contrast, PV and EV71 mutants resistant to GW5074 treatment were not isolated after 12 passages in the presence of GW5074. These results suggested that the target step of GW5074 was much more conserved in PV and EV71 infection than those of metrifudil, N^6-benzyladenosine and NF449, and that the inhibitory effect could not be overcome by the mutations of the viral proteins.

Inhibitory effect of GW5074 is independent of Raf-1, B-Raf and of the interferon response

To examine the possible involvement of the putative cellular targets of GW5074 in its inhibitory effect, we analysed the effect of the MEK/ERK signalling pathway, which is the downstream signalling pathway of Raf-1, on PV infection by using MEK1/2 inhibitors (SL 327 and U0126) (Fig. 5a). After PV infection, clear CPE in the cells treated with MEK inhibitors appeared at 8 h p.i. The cells were completely destroyed at 32 h p.i., as observed for mock-treated cells infected with PV. However, treatment with GW5074 blocked the appearance of CPE in the cells from 8 h p.i. and at least until 32 h p.i. MEK inhibitors had no inhibitory effect on the pseudovirus infection (inhibition indices of 0.30 and 0.27 at 100 μM), in contrast to GW5074 (inhibition index of 6.3×10^{-4} at 25 μM) (Fig. 5b). In addition, we did not observe an inhibitory effect from a MEK1 inhibitor, PD98059, which was included in the drug library (data not shown).

Next, we analysed the effect of putative targets of GW5074 on PV infection by using siRNAs specifically targeting Raf-1, B-Raf, Pim-1, -2, -3, GAK, HIPK2, MST2 and ATF-3 (Fig. 6a). Partial suppression of PV pseudovirus infection was observed for cells treated with B-Raf siRNA02 and with MST2 siRNA03, but not for other sets of siRNA targeting B-Raf and MST2. We analysed the induction of OAS1 and STAT1 mRNA expression in cells treated with siRNA or with GW5074 as an indicator of the interferon response, which could serve as a non-specific cellular response against PV infection (Yoshikawa *et al.*, 2006). Induction of the interferon response was observed in cells treated with B-Raf siRNA02, but not in those treated with other siRNAs or with GW5074 (Fig. 6c). To examine further the role of Raf-1 and B-Raf, we analysed the effect of downregulation of Raf-1 and B-Raf on the sensitivity of RD cells to the inhibitory effect of GW5074 (Fig. 6a and b), and found that downregulation of Raf-1 and B-Raf did not affect the sensitivity of RD cells to GW5074. These results suggested that the inhibitory effect of GW5074 on PV infection did not depend on the MEK/ERK signalling pathway, expression of Raf-1 and B-Raf, or the interferon response, and that at least individual downregulation of previously known *in vitro* targets of GW5074 was not sufficient to show the inhibitory effect.

Table 2. Effect of identified drugs on the infectivity of PV and EV71 strains

Drug	Incubation time of drug (h p.i.)	EV71*					PV			
		BrCr-TR (A)	Nagoya (B1)	C7-Osaka (B4)	1095 (C2)	75-Yamagata-2003 (C4)	Type 1 Sabin	Type 1 Mahoney	Type 2 Sabin	Type 3 Sabin
GW5074	2–9	1.5×10^{-2}	5.8×10^{-3}	3.9×10^{-3}	4.1×10^{-3}	3.6×10^{-3}	2.5×10^{-4}	4.5×10^{-3}	7.7×10^{-4}	7.0×10^{-5}
Metrifudil	2–9	7.2×10^{-4}	1.2×10^{-3}	4.2×10^{-3}	2.2×10^{-3}	1.8×10^{-3}	1.6	ND	ND	ND
N^6-benzyladenosine	2–9	9.5×10^{-4}	9.2×10^{-4}	4.0×10^{-3}	3.2×10^{-3}	1.9×10^{-3}	1.5	ND	ND	ND
NF449	2–9	2.0	0.74	0.71	0.48	1.6	1.8	ND	ND	ND
NF449	0–2	1.6×10^{-1}	7.2×10^{-3}	3.0×10^{-3}	9.1×10^{-3}	4.2×10^{-3}	ND	ND	ND	ND
Mock-treated	0–2 or 2–9	1.0	1.0	1.0	1.0	1.0	1.0	1.0	1.0	1.0

*The genotype of each strain is shown in parentheses.

DISCUSSION

By using a pharmacologically active drug library (LOPAC^{1280} library) with PV and EV71 pseudoviruses, we identified two compounds, metrifudil and NF449, with anti-EV71 activity and one compound, GW5074, with both anti-PV and anti-EV71 activities that suppressed the infection to less than 10^{-4} of that in mock-treated cells. We also found that N^6-benzyladenosine, which is structurally related to metrifudil, efficiently blocked the replication of EV71. For metrifudil and N^6-benzyladenosine, the spacer between the phenyl group and adenosine moiety of this compound seemed critical for the inhibitory effect, because no inhibitory effect was observed for the treatment with N^6-2-phenylethyladenosine (ethyl spacer) and N^6-phenyladenosine (no spacer) (data not shown). The determinants of EV71 mutants resistant to these compounds were identified in the viral protein 2C. Identified mutations were located in the C terminus portion of protein 2C (amino acid positions 325 and 324 for metrifudil and N^6-benzyladenosine resistance, respectively), which is responsible for the appearance of altered membranes in the PV-infected cells by unknown mechanism (Teterina *et al.*, 1997). Mutations in this region were not observed in PV mutants resistant to guanidine hydrochloride, MRL-1237 and hydantoin, which suppress PV replication by inhibiting ATPase activity and/or encapsidation activity of protein 2C (Pfister & Wimmer, 1999; Shimizu *et al.*, 2000; Vance *et al.*, 1997). Therefore, the mechanisms of inhibition by metrifudil and N^6-benzyladenosine via EV71 protein 2C remain to be further studied. NF449 blocked EV71 infection at the steps of binding and/or uncoating, and the determinants of the resistance to NF449 were identified in the viral capsid protein VP1. We observed a partial resistance for BrCr-TR strain against NF449 treatment, which had a positively charged amino acid residue at position 98 in protein VP1 (lysine in BrCr-TR strain and glutamic acid in other strains examined). Amino acid changes responsible for the resistance were located at the BC loop and near the fivefold axis of the virion (Ranganathan *et al.*, 2002). In PV infection, the receptor binding brings a fivefold axis close to the membrane, suggesting a direct function of this site in the uncoating process (Bubeck *et al.*, 2005). Interestingly, a mutation near the fivefold axis has been identified in a mouse-adapted EV71 strain, which affected the binding to the cells (Arita *et al.*, 2008). A polyanionic property of NF449 might suggest an ionic interaction of EV71 with its receptor at the site near the fivefold axis. The direct interaction of these compounds with viral or cellular proteins remains to be further tested.

In contrast to metrifudil, N^6-benzyladenosine and NF449, the inhibitory effect of GW5074 did not allow the emergence of revertants under the conditions examined. GW5074 was originally identified as a Raf-1 inhibitor (Lackey *et al.*, 2000), but also inhibits various kinases *in vitro*, including Pim isoforms (Pim-1, -2 and -3), HIPK2, RIP2, GAK and MST2, and those are considered as more potent targets of GW5074 than Raf-1 (Bain *et al.*, 2007). RIP2 could be strongly inhibited by a p38 inhibitor,

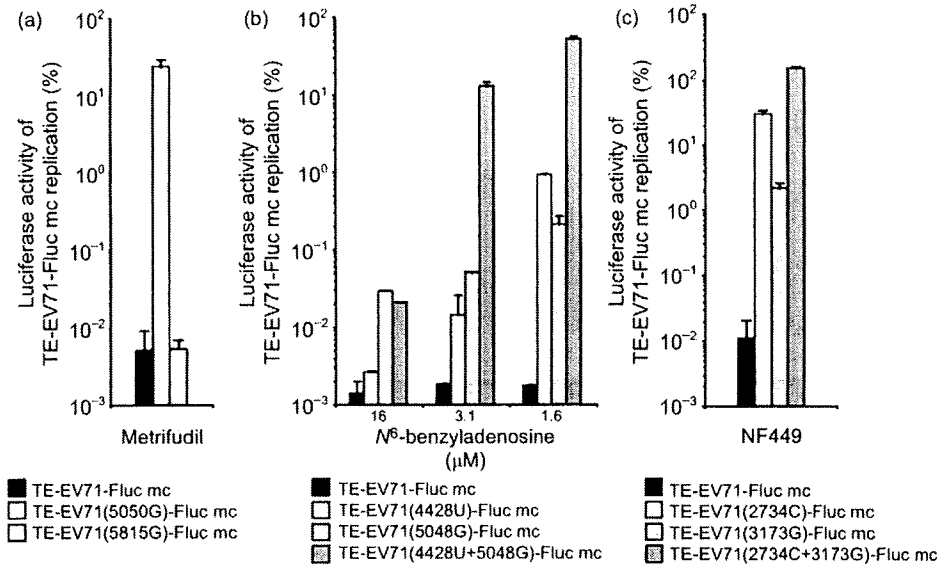

Fig. 4. Characterization of EV71 mutants resistant to identified anti-EV71 inhibitors. Percentage of the pseudovirus replication relative to that in mock-treated cells, which was taken as 100 %, is shown. (a, b) EV71 pseudovirus with a mutation in viral protein 2C was resistant to metrifudil treatment. RD cells were inoculated with 100 IU EV71 pseudovirus in the presence of metrifudil (16 μM) or of N^6-benzyladenosine. (c) EV71 pseudovirus with mutations in viral capsid protein VP1 was resistant to NF449 treatment. RD cells were inoculated with 100 IU EV71 pseudovirus in the presence of NF449 (31 μM).

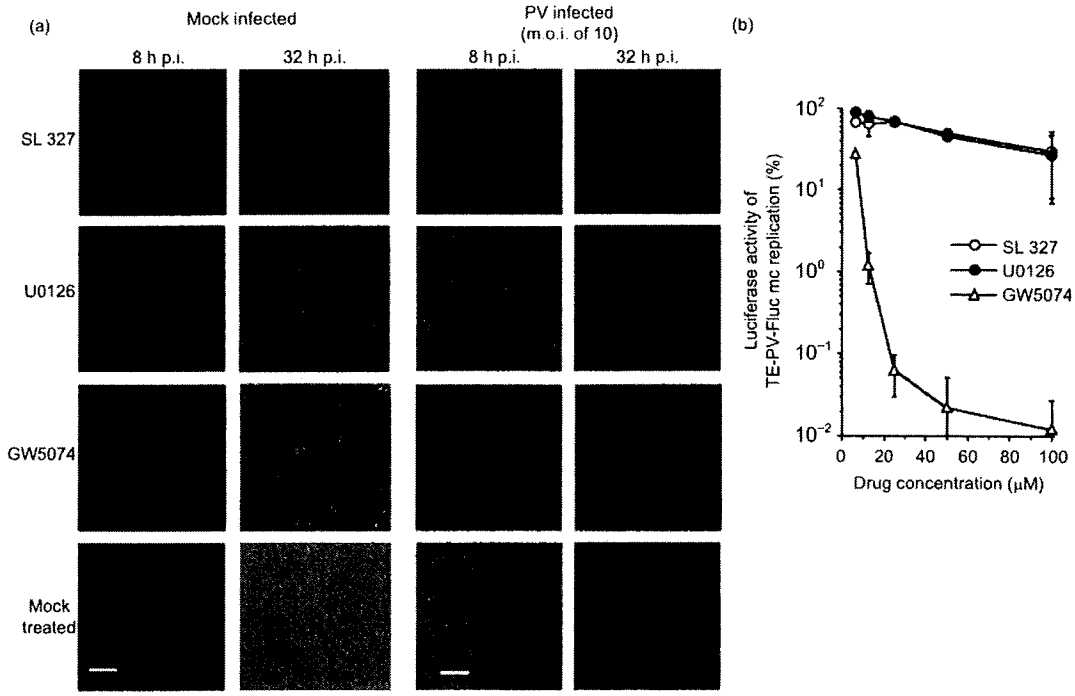

Fig. 5. GW5074 inhibits PV replication independently of the MEK/ERK signalling pathway. (a) Effect of MEK inhibitors (SL327 and U0126) and GW5074 on PV infection. RD cells were inoculated with PV (Mahoney) (at a m.o.i. of 10) in the presence of each drug (25 μM). (b) Effect of MEK inhibitors and GW5074 on PV pseudovirus infection. RD cells were inoculated with 100 IU PV pseudovirus in the presence of each drug. The cells were collected at 8 h p.i. and the luciferase activity in the cells was measured. Bars, 100 μM.

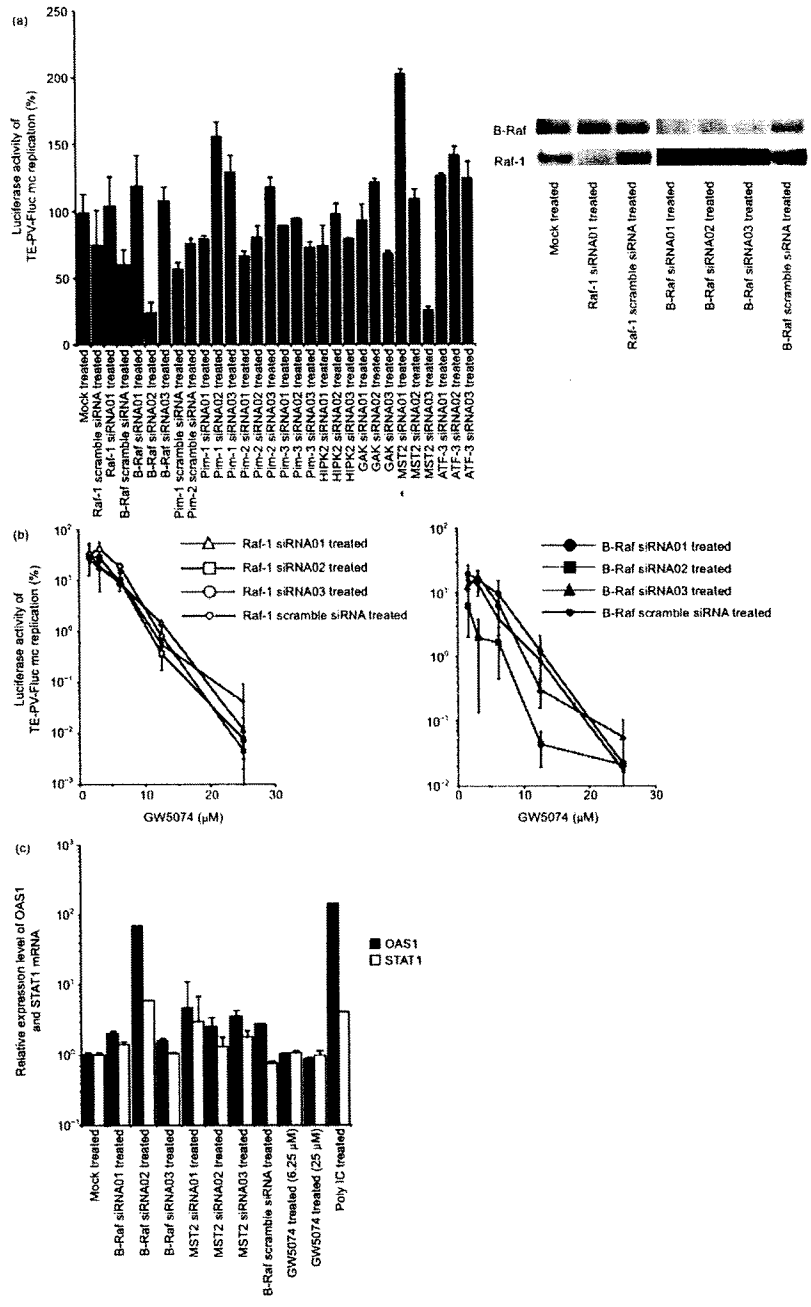

Fig. 6. Effect of siRNA treatment against putative cellular targets of GW5074 on PV replication. (a) Effect of siRNA treatment against putative targets of GW5074 on PV pseudovirus infection. Left panel: RD cells were treated with siRNAs against putative targets of GW5074; the cells were then inoculated with 100 IU PV pseudovirus at 72 h post-transfection. Percentage of the pseudovirus replication relative to that in mock-treated cells at 8 h p.i., which was taken as 100 %, is shown. Right panel: Western blot analysis of Raf-1 and B-Raf in siRNA-treated cells. (b) Effect of downregulation of Raf-1 and B-Raf on the inhibitory effect of GW5074. RD cells treated with siRNAs against Raf-1 (left panel), B-Raf (right panel) and control siRNAs with scramble sequences were inoculated with 100 IU PV pseudovirus at 72 h post-transfection in the presence of GW5074. Percentage of the pseudovirus replication relative to that in mock-treated cells is shown. (c) Interferon response of siRNA- or GW5074-treated cells. The relative expression levels of OAS1 and STAT1 mRNAs in the cells were determined by real-time PCR using β-actin mRNA as the endogenous control normalized by the OAS1 and STAT1 mRNA expression in mock-treated cells. Poly IC-treated cells were taken as positive control of the interferon response.